ABSTRACT

SUI, XINYI. Study of Biodegraded Fabrics containing Reactive Yellow 174: An Analytical Approach (Under the direction of Nelson Vinueza Benitez).

While the invention of reactive dyes promotes the development of textile industry, the waste from production and consumption have placed a significant pressure on the environment. As the world population soars in the last decade, the demand for colored fabrics also increases, which results in an excess of colored fabric waste. The disposal of synthetic dyes has always been a concern for both researchers and entrepreneurs. The current method of disposal is landfill, which mainly involves burying of waste in an open land and after an extended period of time, the fabrics were consumed by microbial such as fungus and bacteria. But what happened to the dye and fabric remain uninvestigated. A major challenge on this kind of study is the limitation of the degraded sample.

Mass spectrometry (MS) has already established its reputation in the analytical chemistry field due to its sensitivity, accuracy, as well as versatility. Through the coupling of High-Performance Liquid Chromatography (HPLC) with MS, a quantitative analysis on the composition of the complexed mixture could be accomplished.

To understand this degradation process, a series hydrolysis reactions on reactive Yellow 174 dye solution and colored fabrics were performed. First, the behavior of this reactive dye under different pH conditions were analyzed by Thin Layer Chromatograph (TLC) and then examined by Time of Flight mass spectrometer. The results show that both of acid and basic condition could produce hydrolysis product but in different form. Based on that, the progress of hydrolysis reaction over time was monitored by Liquid Chromatography-Mass spectrometry (LC-MS). According to the results, the monofluorotriazine group on the dye is more reactive than the vinyl sulfone group. Next, the behavior of the fabrics under different pH conditions

was investigated. Based on these results, another group hydrolysis reactions on fabrics were carried out and monitored by LC-MS. These results showed that alkaline conditions were able to remove the bonded dye from the fabrics. Finally, the characterization of degraded fabrics was carried out by spectrophotometry and Gas Chromatography- Mass spectrometry, which confirmed the loss of dye as well as the presence of textile auxiliaries' residue on the fabrics. Based these results, future work will be focused on the development of enzymatic method and the analysis of potential degraded dye in the soil.

Study of Biodegraded Fabrics containing Reactive Yellow 174: An Analytical Approach

by
Xinyi Sui

A thesis submitted to the Graduate Faculty of
North Carolina State University
in partial fulfillment of the
requirements for the degree of
Master of Science

Textile Chemistry

Raleigh, North Carolina

2017

APPROVED BY:

_____	_____
Nelson Vinueza Benitez	Stephen Michielsen
Committee Chair	

_____
David Muddiman
Minor Member

BIOGRAPHY

Xinyi Sui was born in Hengshui, Hebei Province, China on October 3, 1993. In the year of 2012, he was admitted by Jiangnan University, which is one of best known textile institute in the country. He earned his bachelor's degree in textile chemistry from Jiangnan University in 2016. During his undergraduate years, he used to work on the synthesis as well as the applications of bleaching activator. These experiences pushed him to pursue his Master of Science Degree at North Carolina State University, where his current research focuses on the study on the degradation of reactive dyes using mass spectrometry.

ACKNOWLEDGMENTS

Here I would express my sincere gratitude to my advisor, Dr. Nelson Vinueza, for his visionary guidance, insightful advices and genuine supports in my master program, without which this thesis would not have been accomplished to its least content. Additionally, I would like to thank the help from my Dr. David Muddiman and Dr. Stephen Michielsen. I would also like to thank our group member, Cody Zane, Emily Lichtenberger, Kelsey Boes, Nadia Sultana, and Yufei Chen, all of whom have been always very supportive, helpful and collaborative to me as well as my research work. In addition, I really appreciate the kindness, care and helpful experience offered by COT officers Traci Figura and Amanda Padbury. Finally, I would like to thank my parents for their consistent support on my life and studies at NC State, and all those lovely close friends from 3+X program including Jixin Gong, Lanjun Yin, Ningjun Tong, Runqian Zhang, Shuzhen Wei, Xiaolu Guo, just to name a few. Thanks a lot for all their generous supports whenever and wherever I needed. I feel so blessed to have all of them in my life in the United States.

TABLE OF CONTENTS

LIST OF TABLES……vi
LIST OF FIGURES……vii
1. Introduction ……1
2. Literature Review……2
2.1.Mass spectrometry……....2
2.1.1. History of Mass spectrometry……2
2.1.2. Components of MS system……4
2.1.3. Electrospray Ionization……..7
2.1.4. Quadrupole Mass analyzer……9
2.1.5. Time-of-Flight Mass analyzer……..11
2.1.6. Tandem Mass Spectrometry…….....14
2.1.7. Liquid Chromatography – Mass Spectrometry……17
2.2.Reactive dye……....20
2.2.1. Structural Components of Reactive Dye……...……...20
2.2.2. Reaction between dye and Cellulose……..……22
2.2.3. Hydrolysis of reactive dyes……..25
2.3.Degradation of reactive dye fabrics……27
2.3.1. Chemical reactions on cellulose……...27
2.3.2. Effect of acid on cellulose……28
2.3.3. Effect of base on cellulose……...29
3. Experimental……..31
3.1.Materials……31
3.1.1. Solvents……31
3.1.2. Dyes……31
3.1.3. Fabrics……..31
3.1.4. General Chemicals……...32
3.1.5. Other supplies……..32
3.2.Wet Chemistry……32

3.2.1. Behavior of C.I. Reactive Yellow 174 under different pH condition……..32
3.2.2. Study on the Hydrolysis of Reactive Yellow 174 under alkaline condition…33
3.2.3. Hydrolysis of Reactive Yellow 174 colored fabrics……34
3.2.4. Thin-layer Chromatography……37
3.3.Instrumental analysis……..38
3.3.1. Spectrophotometric analysis……38
3.3.2. Analysis of the behavior of dye at different pH by TOF MS……..39
3.3.3. MS/MS study on the dissociation pathway of C.I. Reactive Yellow 174 and hydrolysis product……...40
3.3.4. LC-MS Analysis……..40
3.3.5. Potential volatile compound detection by GC/MS……..41
4. Results and Analysis……..45
4.1. TLC on the behavior of dye at different pH……...45
4.2. Analysis on the hydrolysis reaction of Reactive Yellow 174 by Mass Spectrometry
4.2.1. TOF MS spectra of Reactive Yellow 174 dye solution at different pH……..46
4.2.2. MS/MS analysis on native Reactive Yellow 174 and its hydrolysis product..54
4.2.3. Reaction Monitoring of on the hydrolysis of Reactive Yellow 174……58
4.2.4. LC-MS Study on the Hydrolysis of undegraded Reactive Yellow 174 fabrics…….62
4.3. Characterization of degraded fabrics ……64
4.3.1. Spectral properties of Reactive Yellow 174 Fabrics with and without degradation …….64
4.3.2. GC-MS spectra on degraded fabrics extraction……...65
5. Conclusion and Future work……..74
6. REFERENCES……..74
7. APPENDICES……...78

LIST OF TABLES

Table 1 Conditions of hydrolysis reactions on dye solution ……..…….32

Table 2 Peak Abundance of the hydrolysis products at different condition……60

Table 3 List of all compounds found in degraded fabrics washing liquids…….72

LIST OF FIGURES

Figure 1 Scheme of parabolic spectrograph……...3

Figure 2 Components in a modern MS system……..5

Figure 3 Conceptual Diagram of Electrospray Ionization (ESI)……...8

Figure 4 Cross section of a Quadrupole with cylindrical approximation……..9

Figure 5 Working mechanism of reflectron…….12

Figure 6 Principle of delayed ion extraction verves immediate extraction…….13

Figure 7 Diagram of one (top) and two (bottom) staged tandem in space MS……14

Figure 8 Diagram of Collision Induced Dissociation……..15

Figure 9 Scheme on the composition of HPLC System…….....17

Figure 10 Separation principle of Liquid Chromatography…….18

Figure 11 (a) Structure of C.I. Reactive Blue 19 ...…..……..20

Figure 11 (b) Structure of C.I. Reactive Orange 35 ……...…….21

Figure 12 Ionization of cellulose…….21

Figure 13 (a) Mechanism of nucleophilic substitution ……...23

Figure 13 (b) Mechanism of nucleophilic addition……..24

Figure 14 (a) Fixation bifunctional reactive dye……..26

Figure 14 (b) comparison in Fixation properties between bifunctional reactive dye and monofunctional reactive dye……26

Figure 15 Chemical structure of cellulose……...27

Figure 16 Acid hydrolysis of cellulose……29

Figure 17 Structure of Reactive Yellow 174……...30

Figure 18 Reactive Yellow 174 solution heated at different pH ……32

Figure 19 Experiment Setup of Reactive Yellow 174 alkaline hydrolysis at different concentration ……..33

Figure 20 Setup of acid treatment experiment on undegraded Reactive Yellow 174 fabrics..35

Figure 21 Picture of degraded (45, 90 days) and undegraded R.Y 174 fabric……38

Figure 22 (a) GC/MS instrument control parameters: page 1…….41

Figure 22 (b) GC/MS instrument control parameters: page 2…….42

Figure 22 (c) GC/MS instrument control parameters: page 3……..43

Figure 23 TLC of Reactive Yellow at different pH before and after heating……..45

Figure 24 (a) Full spectrum of Reactive Yellow 174 solution heated at native pH…….46

Figure 24 (b) Experimental isotropic distribution of triply charged Reactive Yellow 174….46

Figure 24 (c) Experimental isotropic distribution of doubly charged sodiated Reactive Yellow 174 ……..47

Figure 25 (a) Full spectrum of Reactive Yellow 174 solution heated at pH 3……48

Figure 25 (b) Experimental spectrum of protonated and sodiated hydrolyzed product in MFT group……48

Figure 26 Full spectrum of Reactive Yellow 174 solution heated at native pH 6……...48

Figure 27 Full spectrum of Reactive Yellow 174 solution heated at pH 7……..49

Figure 28 (a) Full spectrum of Reactive Yellow 174 solution heated at pH 10……..50

Figure 28 (b) Zoom in spectrum showing the inference of isotropic distribution between m/z 407.5 and 419.5 ……..50

Figure 29 (a) Full spectrum of Reactive Yellow 174 solution heated at pH 12……..52

Figure 29 (b) Zoom in spectrum of protonated and sodiated Reactive Yellow 174 hydrolysis product in Vinyl Sulfone and Triazne group……...52
Figure 29 (c) Structure of protonated hydrolysis product in Vinyl Sulfone and Monofluorotriazine group……53
Figure 29 (d) Structure of sodiated hydrolysis product in Vinyl Sulfone and Monofluorotriazine group……53
Figure 30 (a) MS/MS spectrum of doubly charged native Reactive Yellow 174 ……...54
Figure 30 (b) MS/MS spectrum of doubly charged Reactive Yellow 174 hydrolysis product……55
Figure 30 (c) MS/MS spectrum of doubly charged Reactive Yellow 174 hydrolysis product in Vinyl Sulfone and monofluorotriazine group ……..56
Figure 30 (d) Structure of product ion with m/z 348.5……56
Figure 31 (a) DAD chromatogram of hydrolysis of Reactive Yellow 174 at different time...57
Figure 31 (b) LC-MS spectra on Hydrolysis of Reactive Yellow 174 at different time…….59
Figure 31 (c) LC-MS spectra on Hydrolysis of Reactive Yellow 174 with different alkaline concentration……61
Figure 32 (a) DAD Chromatogram on the hydrolysis of Reactive Yellow 174 fabric at different pH condition……..62
Figure 32 (b) LC-MS on the hydrolysis of Reactive Yellow at different pH condition……..62
Figure 32 (c) LC-MS on the alkaline hydrolysis of Reactive Yellow 174 at different concentration……63
Figure 33 Absorption Curve before and after the Degradation……...64

Figure 34 (a) GC Chromatogram of degraded white fabrics washing liquid……..65

Figure 34 (b) MS spectrum of peak at 15.236 minutes and system match……..66

Figure 34 (c) MS spectrum of peak at 15.464 minutes and system match……..66

Figure 34 (d) MS spectrum of peak at 16.519 minutes and system match……..67

Figure 34 (e) MS spectrum of peak at 22.853 minutes and system match……..67

Figure 35 (a) GC Chromatogram of degraded Reactive Yellow 174 fabrics washing liquid..68

Figure 35 (b) MS spectrum of peak at 12.047 minutes and system match……..69

Figure 35 (c) MS spectrum of peak at 15.236 minutes and system match……..70

Figure 35 (d) MS spectrum of peak at 22.842 minutes and system match……..70

1. Introduction

Synthetic dyes have been playing an important role in the modern textile industry since its invention by William Henry Perkin in 1856 *(1)*. A lot of efforts has been invested into the development of new synthetic dyes with better color fastness and more available colors. One representative of this kind of innovation is the invention of the reactive dye in the 1950s by Imperial Chemical Industries.*(2)* Unlike direct or disperse dyes which mainly rely on physical absorption, reactive dyes use a chemical reaction to create a covalent bond between fabric (cotton or wool) and dye, which gives them better colorfastness than direct or disperse dye.

While the invention of reactive dyes has significantly promoted the development of textile industry. The degradation of these synthetic dyes has always been a concern for both researchers and entrepreneurs. As the world population soars in the last decade, the demand for colored fabrics also increases, which results in an excess of colored fabric waste. The current method of disposal is landfill, which mainly involves burying of waste in an open land and after an extended period of time, the fabrics were consumed by microbial such as fungus and bacteria.*(3)* Now the question will be, what happened to the dye?

In order to investigate this question. This project will be divided into three phases. At phase one, Thin Layer Chromatography and Time of Flight mass spectrometry were used to study the behavior of Reactive Yellow 174 dye molecule at different pH. Meanwhile, Liquid Chromatography – Mass Spectrometry (LC-MS) will be introduced to monitor the progress of hydrolysis reaction. Based on the results from phase one, the hydrolysis reaction were performed on fabrics containing Reactive Yellow 174. The solutions obtained from fabrics were treated at different conditions, acid and base, follow by the analysis LC-MS. Then, at

phase three, non-destructive analyses on degraded fabrics such as spectrophotometry and Gas Chromatography- Mass Spectrometry were performed on degraded fabrics to characterize the changes in its properties. Results from this project will greatly assist the development of analysis method on degraded fabrics, which features the intact removing of the dye while minimizing the hydrolysis.

2. Literature Review

2.1. Mass spectrometry

2.1.1. History of Mass spectrometry

As a saying goes *(4)*, the history of chemistry was promoted by peoples' desire to find or build something could measure mass accurately and easily. An example of this is the establishment of mass spectrometry (MS) and the development of mass spectrometer. From Joseph John Thomson's discovery of electrons to the development of Orbitrap system by Makarov, the advancing of MS has always been pushed by the joint forces of scientific discovery and engineering innovation. *(5)*

The first milestone in the development of mass spectrometer was the discovery of the electron by Joseph John Thomson in 1906. In his second experiment in 1912, he built a device that could bend the direction of the electron beam by applying a voltage to it and detect this change in direction by an electron-sensitive capture plate. This device, which is shown in Figure 1, is called parabolic spectrograph and it is now believed to be the world's first mass spectrometer.*(6)* Following the discovery by Thomson, researchers started to apply this new technique to investigate the nature of elements. In 1918, Arthur Jeffrey Dempster developed the first mass spectrometer with electron ionization source, which is still the most popular

ionization method today.*(5)* Francis W. Aston obtained the world's first mass spectrograph in 1919 and used it to determine the atomic mass of different elements. By the time of World War II, based on Dempster' design, Alfred Otto Carl Nier was able to isolate Uranium-235 for the Manhattan Project with his improved mass spectrometer. In the year of 1946, W. Stephens published a review study on the potential of building an instrument that could send a package of ions for ion source to fly down a vacuum tube and its mass-to-charge ratio could be determined by measuring the time the ion takes to fly in the tube. This conceptual design of instrument was later proved to be the theoretical base of Time-of-Flight (TOF) mass spectrometer, which is one of the major mass analyzers today.*(7)* The first commercial TOF instrument was developed by Bendix Corporation in 1950. *(8)*

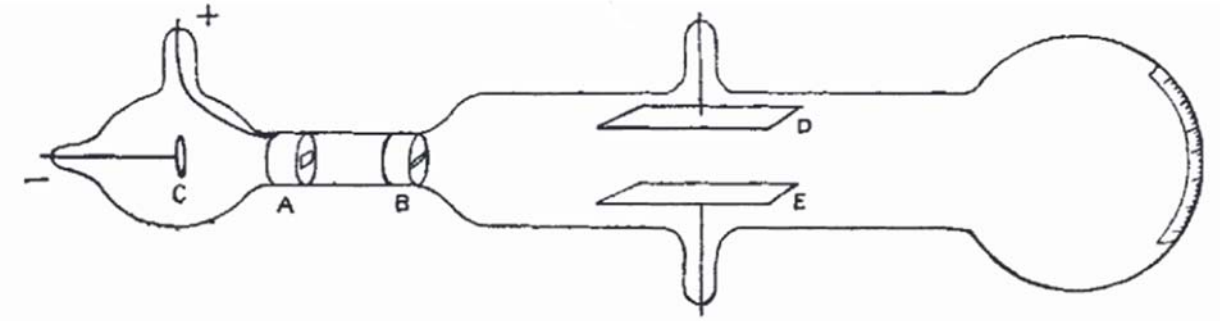

Figure 1 Scheme of parabolic spectrograph

By the time of the 1950s, half a century after J.J Thomson's discovery of the electron, a lot of novel theories have been proposed on the development of mass spectrometry but due to a lack available electronics, these innovative ideas would have to wait several decades before the development of the corresponding instrument. For instance, the theory of orbital trapping was discovered by K. H. Kingdon in 1923, in this study, he proposed a design of Orbitrap tube

with a cylindrical anode and calculated the parameters needed to manipulate the ions.*(9)* But the engineering and electronics at that age was not able fully to utilize this discovery until the 1990s when Alexander Makarov and his team started to develop an Orbitrap mass spectrometer.*(10)* In the year of 2005, 70 years after Kingdon's discovery, the first commercialized Orbitrap instrument was announced by Thermo Scientific. *(5)*

Another metric reflecting the development of a mass spectrometer is the increasing of resolving power, which represents the capability of a certain instrument to separate isotropic distribution. The parabolic mass spectrograph built by J.J Thoman had a resolving of 13 and the two-stage mass spectrograph built by Aston had a resolving power of nearly 100, which is barely enough for the study of the isotopic composition of a certain element. But after a century of development, nowadays with Fourier Transform Ion Cyclotron Resonance mass spectrometry (FT-ICR-MS), the researchers could have a resolving power of 1,000,000, where the instrument could resolve the whole isotropic distribution of an entire protein.*(11)*

2.1.2. Components of MS system

Figure 2 shows a conceptual diagram of a mass spectrometer, nowadays a complete MS system is made up of five components: Sample introduction, Ionization Source, Mass analyzer, Detection System, and Data system.*(12)*

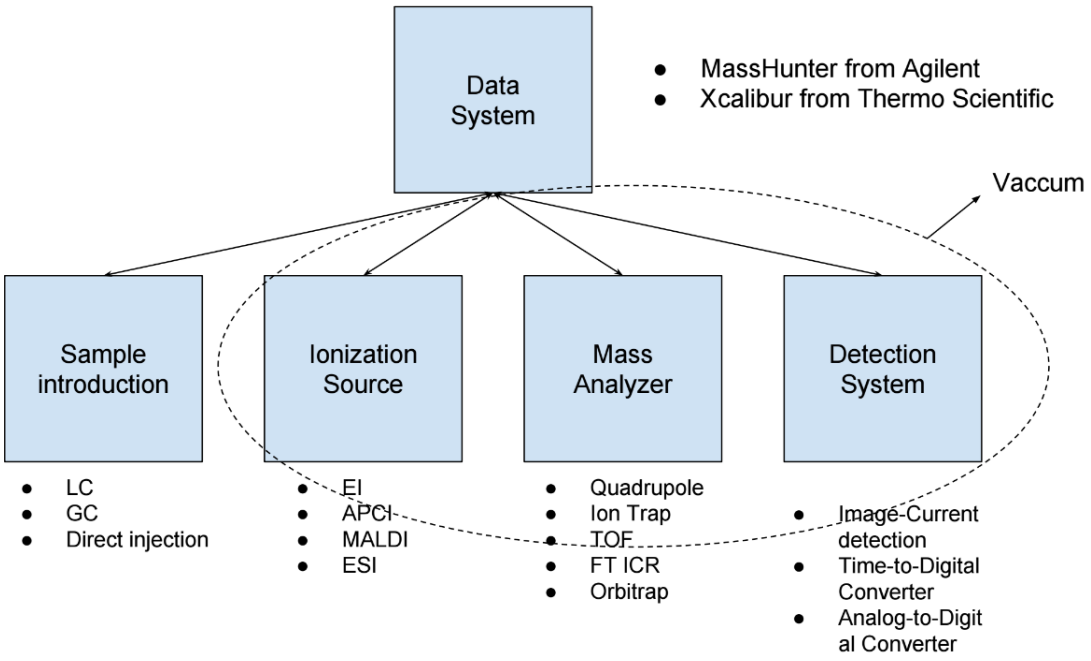

Figure 2 Components in a modern MS system*(4)*

Sample introduction is the entry of analyte and the interface between the mass spectrometer and other analytical methods. Usually, when dealing with complexes mixtures, the coupling with chromatographic methods with MS is preferred, such as Gas Chromatography (GC) and High-Performance Liquid Chromatography (HPLC). After the separation by the column, each chemical will be separated so that by the time it come out from the column and reaches the detector, a clear spectrum could be obtained for each component.

After the introduction of the sample, the analyte enters the ionization source, the molecules have to be charged so it could be maneuvered by electrical or magnetic field. Currently, Electron Ionization (EI), Chemical Ionization (CI or APCI), Atmospheric Pressure Photoionization Ionization (APPI), Matrix-Assisted Laser Desorption Ionization (MALDI), and Electrospray Ionization (ESI) are usually used as ionization sources. The selection of

ionization method is based on the nature of the analyte. For example, if the sample of interest is very volatile, EI is preferred but if the subject has large molecule weight like peptide or small protein, ESI would be better since it features multiple charging and almost no fragmentation.

After ionization, the stream of analyte ions goes into the mass analyzer. Currently, there are two types of mass analyzer: scanning and pulsed. In scanning mass analyzers such as the quadrupole and the ion trap, ions with different m/z values are detected successively along a time scale. While in pulsing mass analyzers such as Time-of-Flight (TOF), FT-ICR and Orbitrap, the detection was achieved simultaneously. Among them, quadrupole has the lowest resolving power at around 1000 to 2000 while FT-ICR has a resolving power at the level of millions. The major factor, however, in the selection of mass analyzer is not just resolving power but also the objective of the research. Ideally higher resolving power would provide more information but it also means additional cost on instrument and maintenance. An example of this is FT-ICR, which use a magnetic field to create cyclotron motion in ICR cell. But this requires the use of liquid helium to maintain the superconductive status at a temperature below 5 Kelvin. As a result, only a small number of research facilities around the globe have FT-ICR instrument and quadrupole mass analyzer still takes up a great proportion of the mass analyzers used today. *(12)*

In today's mass spectrometer, detection systems are usually built-in with the mass analyzer. The function of detection is to pick up the ions traveling out of mass analyzer and produce a signal. Usually, in the form of analog current, this signal was then converted to digital signal, which could be processed and stored by a data system. In addition to data

management, current data system, which is essentially a package of different software from the manufacturer, could also monitor and control the acquisition of data.

2.1.3. Electrospray Ionization

Electrospray Ionization (ESI) is one of the major ionization method in today's MS instruments. Compared with other ionization methods, ESI has its unique advantages. First of all, it is, by far, the softest ionization method, which means that unlike EI or APCI, where the analytes could be fragmented in certain circumstances, the chemical structure of the sample could be almost perfectly maintained. And it is capable of producing multiple charged ions, which not only increases the dynamic range of the analyzer but also reduce mass measurement error by a factor of 1/z, where z represents the number of charges. As is shown in Figure 3, the ionization process could be demonstrated by a three time point. At t1, the accumulation of charge forms Taylor Cone and ions are drawn toward the direction of the mass analyzer by an electric field. At t2, parent droplets start to emerge as the drag force exceeds the surface tension. These droplets collide with gas molecules that drive the evaporation of the solvent. At t3, the droplets are significantly reduced in their radius due to the evaporation of the solvent and the precursor droplets start to produce offspring droplets. The molecular ion then travels through the heated metal capillary that goes further into the mass analyzer. Regarding the origin of molecule ion, two models were proposed. The Charge Residue Model proposed by Dole suggests that there is a threshold called Rayleigh limit when the columbic force of the droplet exceeds its surface tension and forms offspring droplets. These offspring droplets then undergo further solvent evaporation and experience a columbic fission again. This process continues until there is on average one analyte molecule per droplet with some charge. The

remaining solvent evaporates leaving the charge deposited on the molecule. Another model, the Ion Evaporation proposed by Iribarne and Thomson suggests that the precursor droplets undergo columbic fission when they reach the Rayleigh limit and give rise to offspring droplets. These offspring droplets, rather than continuing to undergo columbic fission, will be affected by the electric field on the surface. As a result, the columbic stress in the droplet is relieved by ejection of molecular ions. Compared with Charge Residue Model, this model can account for the observed mass spectra of molecules with different physicochemical properties.*(13)*

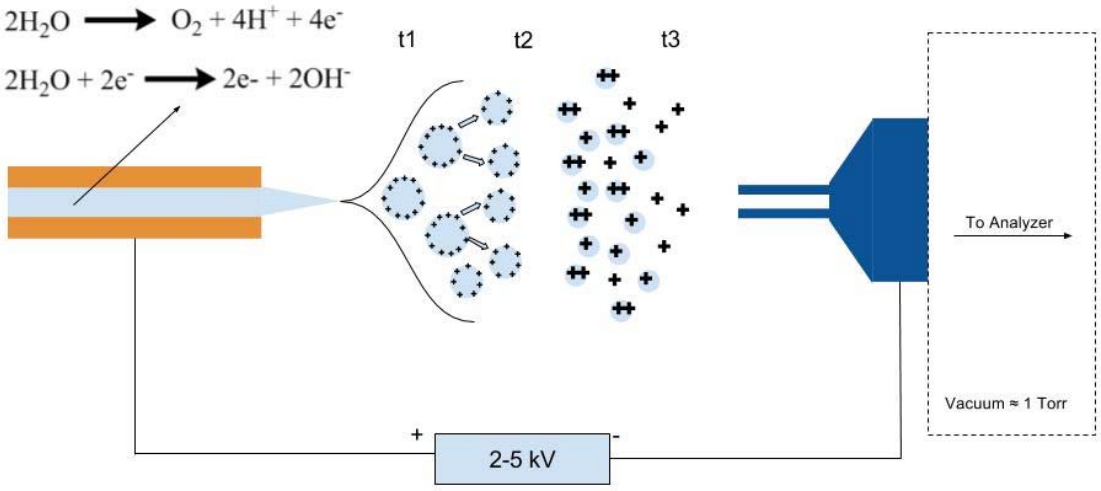

Figure 3 Conceptual Diagram of Electrospray Ionization (ESI)

2.1.4. Quadrupole mass analyzer

As is shown in Figure 4, a quadrupole mass analyzer is made up by four hyperbolically shaped metal rod placed as a square. Each pair of opposite-facing rods extending in Z direction

was connected to one end of the power supply, which means that each pair of opposite rods, will have the same electric potential. The power supply was composed by a Direct Current (DC) module and an Alternating Current (AC) module.

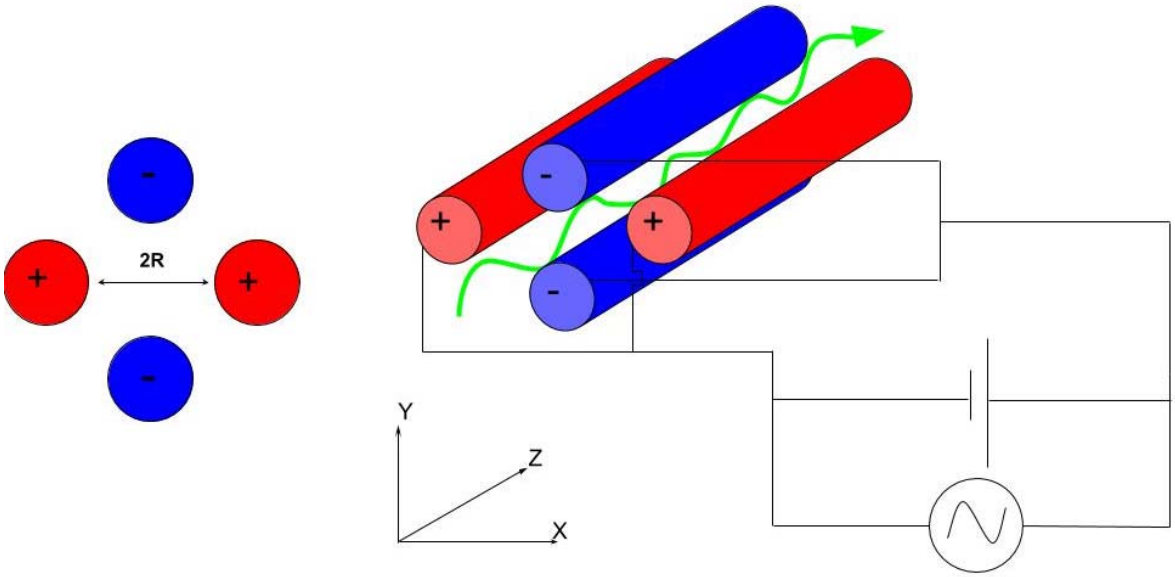

Figure 4 Cross section of a Quadrupole with cylindrical approximation

The working mechanism of quadrupole involves using two pairs of cylindrical rods as "mass filter". As is shown in Figure 4, in the field of positive-charged rods, only ions whose m/z is higher than the threshold could pass through and the in the field of negatively-charged rods, only ions whose m/z is lower than the threshold could pass through. As a result, at a specific time point, only a small range of ions could pass the quadrupole and be detected. According to the simplified Mathieu Equations which is shown in (1), the threshold of each pair of rods was determined by a DC related parameter *a* and an RF (Radio Frequency) related parameter q. By changing these two parameters over time, a scanning of a wide range of m/z could be achieved.

$$a = \frac{8eU}{(m/z)\omega^2 r_0^2} \, q = \frac{4eV}{(m/z)\omega^2 r_0^2} \quad (1)$$

Besides mass filtering in two sides, the quadrupole could perform other functions by changing the power input. By switching off one pair of rods, the quadrupole could select all ions above or below a certain value. If the DC voltage is set to zero, the quadrupole would not be able to filter out ions. Instead, all the ions are confined to travel along the centerline of the quadrupole. In this mode, the quadrupole is called ion guide and it would focus the ion beam and reduce its kinetic energy distribution before it enters another mass analyzer such TOF, FT-ICR, or Orbitrap.

2.1.5.Time-of-Flight Mass analyzer

The TOF was first developed by Cameron and Eggers in 1948,*(14)* and the first commercial TOF was developed by Wiley & McLaren in 1953.*(15)* By that time TOF only have limited resolving power (lower than Quadrupole at that time) due to a spread of initial kinetic energy. During the 1970s, the improvement in electronics and the invention of reflectron by Mamyrin in 1973, enhanced the resolving power of TOF. *(16)*

The working mechanism of TOF involves sending a package of ions, which is generated either by a pulsing ionization source (MALDI) or by chopping up the flow of continuous ionization (ESI), into a highly-vacuumed tube with the same amount of kinetic energy (KE) and measure the arrival time of each ion. According to equation (2) to (4), the time it takes for an ion to reach the detector is proportional to m/z value but if there is an initial spread of kinetic energy, ions with a same m/z value would have a difference in flight time which broadens the peak and decreases the resolving power.

$$KE = zeU_{ex} = \frac{1}{2}mv^2 = \frac{1}{2}m(\frac{dx}{dt})^2 \quad (2)$$

$$m/z = 2eU_{ex}\frac{\Delta x^2}{\Delta t^2} \quad (3)$$

$$\Delta t = t_{arrival} - t_0 = \Delta x\sqrt{\frac{m}{2zeU_{ex}}} \quad (4)$$

In current TOF mass analyzers, the reflectron and delayed ion extraction are introduced to minimize the influence of initial kinetic energy spread. A diagram of the working mechanism of the reflectron is provided in Figure 5. When two ions with the same m/z but different initial kinetic energy (KE) enter the TOF, and if the linear detector was used, those two ions will arrive at a different time which results in a loss of resolving power, but with reflectron, the one with higher KE will have to travel an extra distance in the reflectron, which in the end balances the difference in KE and makes them arrive at the same time.

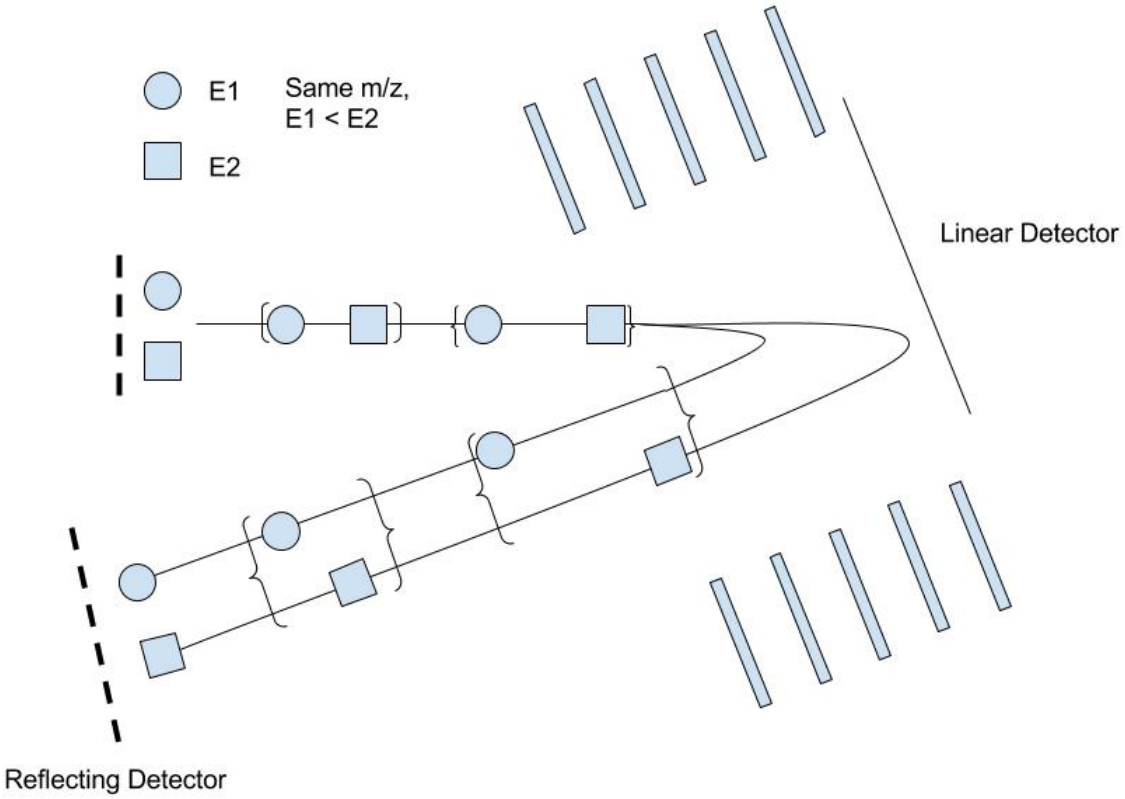

Figure 5 Working mechanism of reflectron

Another technique used to deal with the kinetic energy distribution is delayed ion extraction, which is also called time-lag focus or pulsed ion extraction. The principle of it is shown in Figure 6. Without delayed extraction, the ions get accelerated by the electrical field as soon as they were produced from the ionization source so there will be considerable kinetic energy spread. By delaying time of the extraction, the ions get "cooled down" by being shaken in the electrical field as well as separate out to reduce the chance of hitting each other and fragments.*(13)*

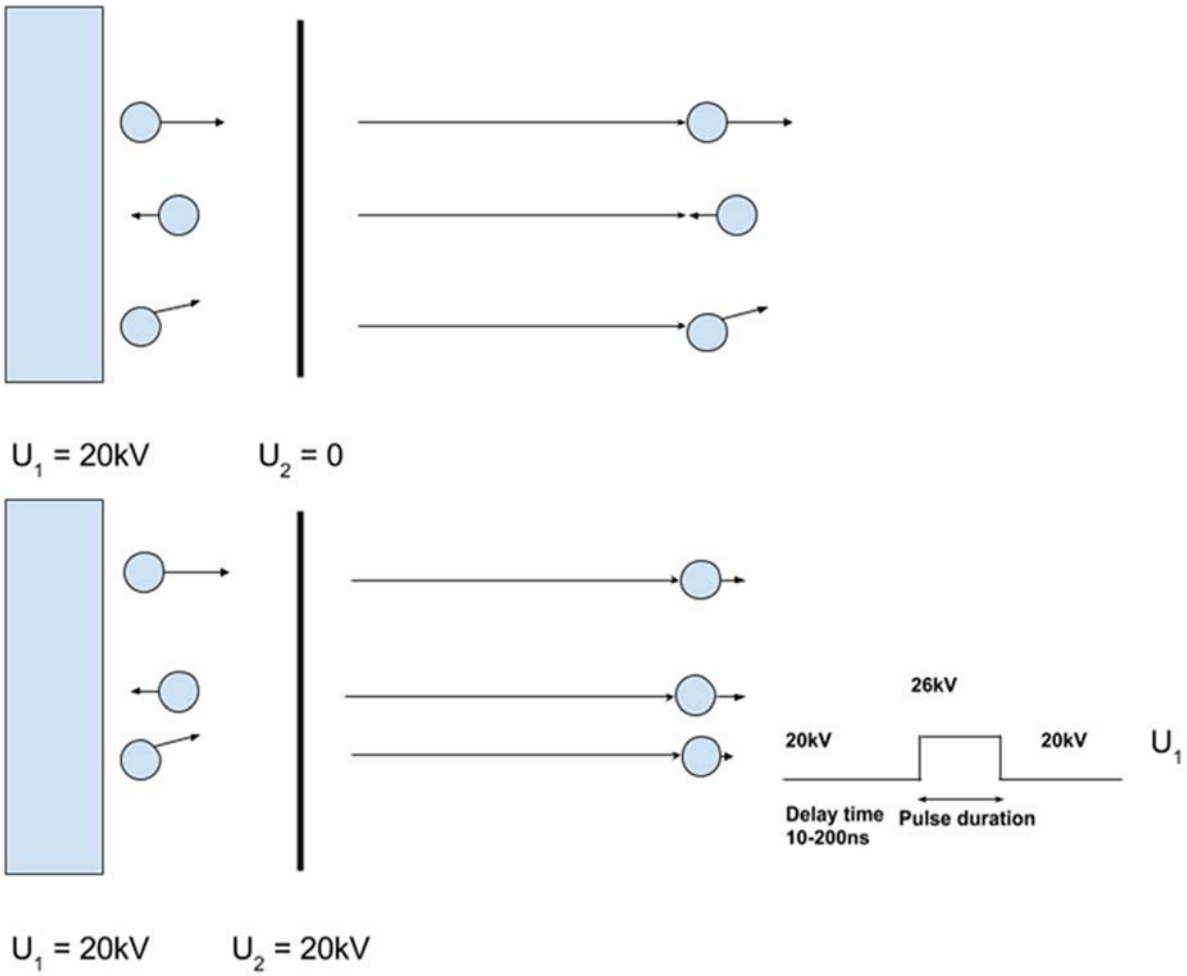

Figure 6 Principle of using delayed ion extraction to reduce kinetic energy distribution

2.1.6.Tandem Mass Spectrometry(MS/MS)

By definition, Tandem Mass Spectrometry means the coupling of multiple (at least two) mass spectrometer to break the molecule and obtain structural information.*(17)* Based on this definition, tandem MS could be divided into two classes: tandem in space and tandem in time. The difference between these two classes is directly related to the instrumentation. In a tandem-in-space capable instrument such as quadrupole Time-of-Flight and triple quadrupole, there is a limitation on how many times the ion could be fragmented. For example, in a triple

quadrupole MS, the target ion is selected in the first quadrupole, then fragmented in the second quadrupole, and detected at the third one. If there is a need to another level of fragmentation, two additional quadrupole has to be installed. Figure 7 shows the diagram of one stage tandem MS in space and two-stage tandem MS in space. The Q represents quadrupole that is assigned to select and detect the ions and q represents the dissociation chamber.

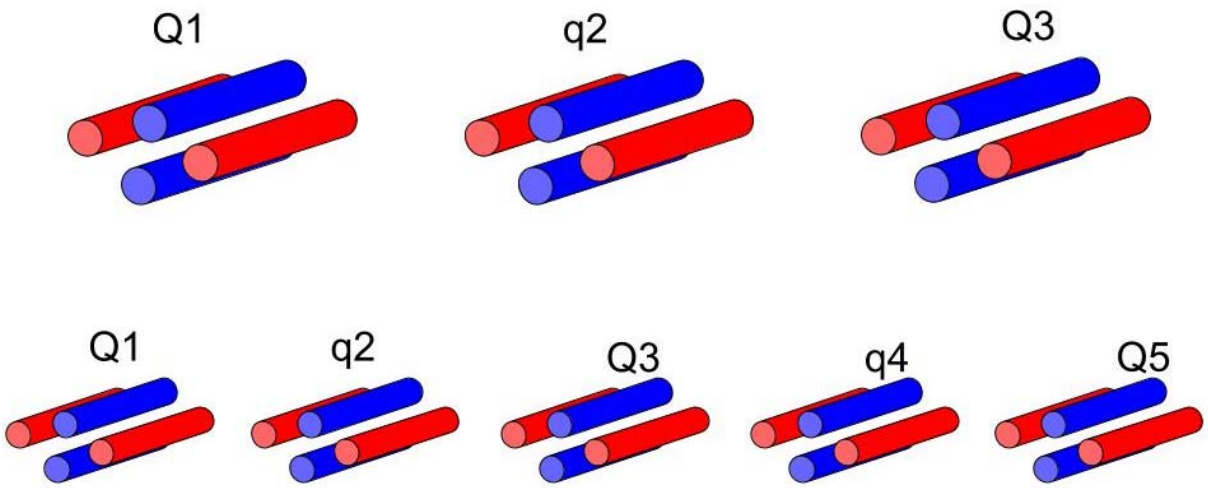

Figure 7 Diagram of one (top) and two (bottom) staged tandem in space MS

On the other hand, a tandem in time mass spectrometer such as quadrupole ion trap and FT-ICR often does not subject to the limitation of fragmentation stages. In this type of instrument, the ion will be trapped in a collision cell and could be fragmented repeatedly until a desired level of dissociation was reached. In theory, this type of instrument could perform MS^n, which means that the in-depth structural information of the target molecule as well as its offspring fragmentation.

Collision-Induced Dissociation (CID), also called Collision-activated Dissociation (CAD) is one of the most common dissociation technique in tandem mass spectrometry. In principle, it involves the inelastic collision between the target molecule and neutral gas molecule. Regarding the mechanism of CID, the revised Rice–Ramsperger–Kassel–Marcus (RRKM) theory was proposed to describe this process. *(18)* According to this theory, a proportion of the kinetic energy could be transferred into the internal energy of the precursor ion. This additional energy soon gets dispersed via redistribution among all the vibration modes of the molecular structure and thus increases the total potential energy level in the system. As soon as the potential energy reaches the threshold, the molecule starts to undergo unimolecular dissociation, which produces product ions via a series of competitive reactions. Figure 8 shows a diagram of this process.

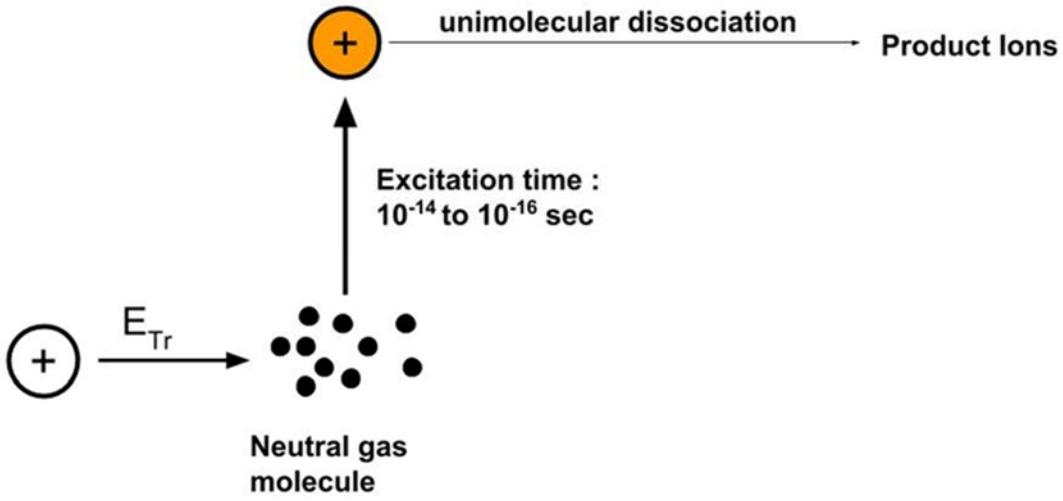

Figure 8 Diagram of Collision Induced Dissociation

$$E_{cm} = E_{TR} \times \frac{m_t}{m_t + m_i} \quad (5)$$

Regarding the collision efficiency of CID, as is shown in equation (5), there are several factors affecting the amount of energy (E_{cm}) transferred during this process: kinetic energy of ions E_{TR}, mass of gas target m_t, and mass of the ion m_i. On one hand, according to this equation, the product ion yield would increase as the kinetic energy and target mass increase. To achieve the same level of energy transfer, an ion with higher molecular weight would require a higher kinetic energy than the ion with low molecular weight.

2.1.7. Liquid Chromatography

Despite the high capability of mass spectrometry, its applications were limited by a series of challenges one of which is the complexity of spectrum brought by the composition of sample mixture. Specifically, the instrument may not have enough resolving power to detect the ion of interest from other ions in the mixture and the peak of interest may have a chance of interfering with each other.*(19)* One effective way to tackle this challenge is the introduction of chromatography. Usually gas or liquid chromatography is used to separate the components of a mixture, as away to enhance characterization of the analytes of interest.

A modern High-Performance Liquid Chromatography (HPLC) system is usually made up of three major components: stationary phase, mobile phase, and detection system.*(20)* A scheme of the composition of HPLC system was provided in Figure 9. Two solvent flows, served as mobile phase, passed the degasser to remove the gaseous residue and entered the sampler, where the analyte is injected into the system and mixed with the solvent flow. After that, the liquid flow goes through the column, which would be maintained at a desired temperature before the introduction of the analyte, and then reaches different detectors such as Diode Array Detector (DAD) before being going into the waste bottle.

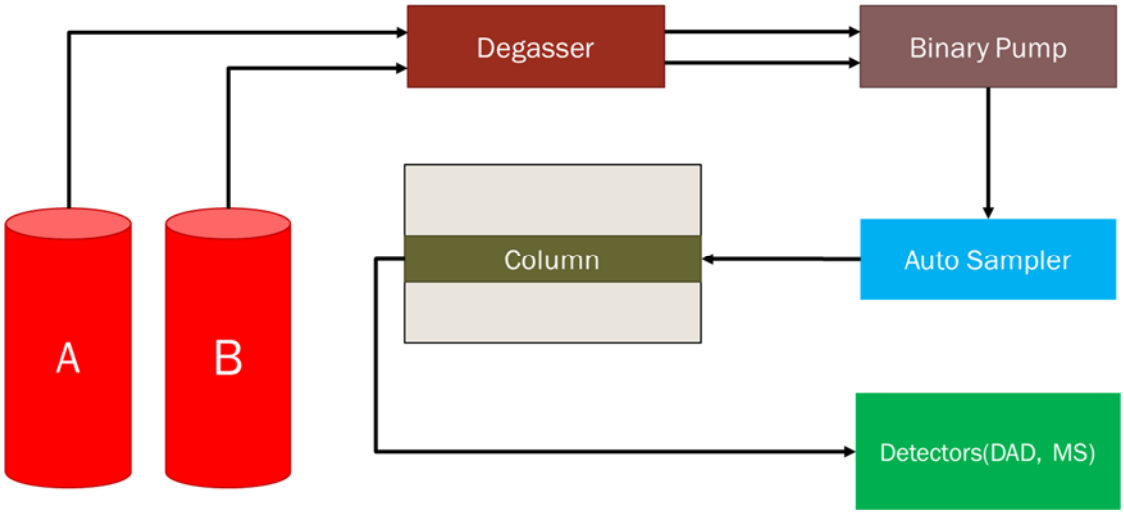

Figure 9 Scheme on the composition of HPLC System

A diagram of the separation principle of liquid chromatography is provided in Figure 10. A mixture containing two components A and B are transported into the column by mobile phase. As the mixture goes through the column, the velocity of each of the components are reduced by their different affinity to the stationary phase. This creates a difference in their actual final velocity which eventually results in a variation in their retention time. For instance, in this diagram, component A has a higher affinity for the stationary phase than to the mobile phase while component B has a higher affinity to the mobile phase. As a result, component A will experience a bigger "drag force" than component B and it will have a lower velocity than B. And since the length of the column is fixed for a certain system, this difference in velocity will come down to a deviation in retention time. *(21)*

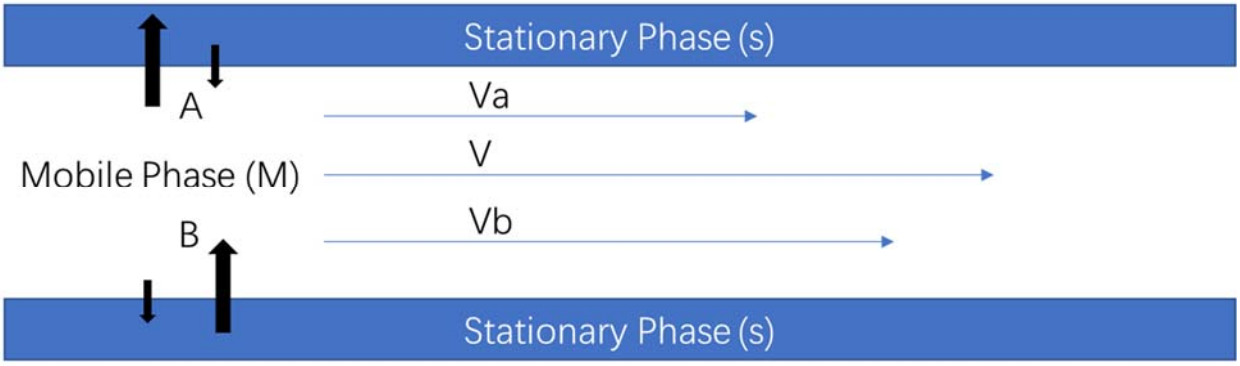

Figure 10 Separation principle of Liquid Chromatography

Regarding the composition of solvent system in LC system, there are two kinds of elution methods: isocratic and gradient elution.*(21)* In isocratic elution, the composition of mobile phase doesn't change over time. Although gradient elution has a higher capability than isocratic elution, it has a number of disadvantages such as time-consuming, difficult to transfer between different systems and detector compatibility problem. So in most cases, the analysis of mixture will start with isocratic elution and then move to gradient elution if isocratic elution could not provide a satisfactory separation.

Another benefit of coupling HPLC with MS is that it enhances the ionization efficiency of some ionization source like ESI. The introduction of HPLC could be helpful for ESI in many ways. For example, it could reduce the flow rate in the system and thus promote the production of smaller droplets at a lower speed. After the mixture gets separated by the column, by the time it reaches the ionization source, each component will be concentrated within its peak width. Since ionization efficiency in ESI could be effected by the concentration of the analyte, this concentration effect brought by HPLC would considerably enhance the ionization efficiency of ESI. *(20)*

2.2. Reactive dye

2.2.1. Structural components of reactive dye

Synthetic dyes have been playing an important role in the modern textile industry since its invention by William Henry Perkin in 1856.*(1)* A lot of efforts has been invested in the development of new synthetic dyes with better color fastness and more available colors. One representative of this kind of innovation is the invention of the reactive dye in the 1950s by Imperial Chemical Industries. Unlike direct or disperse dyes which mainly rely on physical absorption, reactive dyes use a chemical reaction to create a covalent bond between fabric (cotton or wool) and dye, which gives them better fastness than direct or disperse dye.

The structure of a reactive dye could be divided into four main components: chromophore (D), bridging group (B), reactive group (Re), and solvation group(S). A typical structure of reactive dye could be expressed as S-D-B-Re. Among them, the reactive group is the most critical one not only because it ensures the chemical bonding between dye and fiber, it also determines the conditions for fixation process. For example, reactive dyes with vinyl sulfone (VS) group will have a relative lower working temperature (50 to 70 degree Celsius) compared with those with monochlorotriazine (MCT) group (70 to 90 degree Celsius). Reactive dyes with a dichlorotriazine group will have even lower working temperature than those with vinyl sulfone group because of the presence of additional leaving group. *(22)*

The structure of two reactive dyes is provided in Fig 11 (a) and (b). Despite their difference in structure, both of them match the general structure of the reactive dyes. They have different chromophore (anthraquinone or azo group) and different reactive group (vinyl sulfone or monochlorotriazine), but they have the same bridging groups (-NH-) and solubility

(-SO_3) groups.

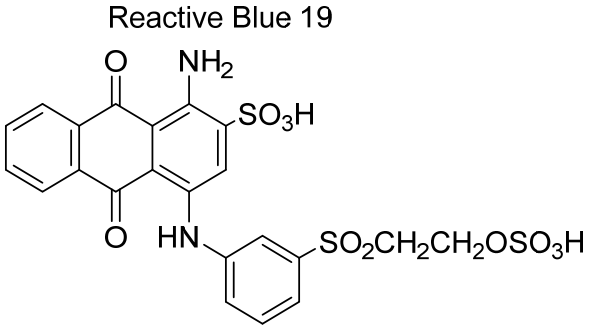

Chemical Formula: $C_{22}H_{18}N_2O_{11}S_3$
Exact Mass: 582.0073

Figure 11 (a) Structure of C.I. Reactive Blue 19

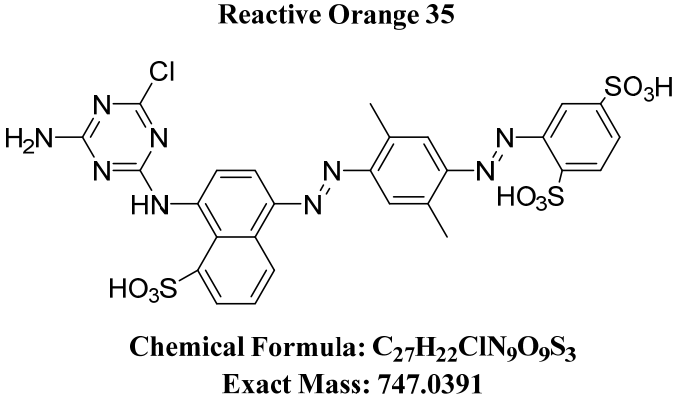

Chemical Formula: $C_{27}H_{22}ClN_9O_9S_3$
Exact Mass: 747.0391

Figure 11 (b) Structure of C.I. Reactive Orange 35

2.2.2. Reaction between Reactive dye and cellulose

The mechanism of the chemical reaction between the fixation processes of has been studied intensively.*(22, 23)* There are two sets of reactions involved in this process: the deprotonation of cellulose and the fixation of dye. Figure 12 shows, the hydroxyl group at the end of each cellulose polymer chain will lose a proton and create a stronger nucleophile in the presence of alkaline solution. The degree of deprotonation increases as the concentration of

base increases. Essentially, this reaction could be considered as a kind neutralization where the cellulose works as a weak acid.

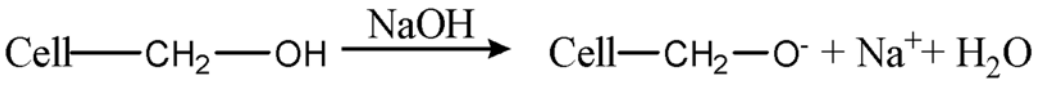

Figure 12 Deprotonation of cellulose

Following the generation of cellulose anion is the fixation of dyes onto the cotton fiber, which essentially is the reaction between cellulose anion and the reactive group in the dye. In this process, depending on different reactive groups, there are majorly two kinds of reactions: nucleophilic aromatic substitution and nucleophilic addition. The mechanism of each kind of reaction is presented in Figure 13(a) and 13(b).

In nucleophilic aromatic substitution, reactive dyes with triazine group will lose chlorine as the leaving group, which increases the density of positive charge. As a result, the cellulose anion will have a greater chance of bonding to the ring. This creates a covalent bond between the dye and the cellulose. A couple of factors will affect the reactivity of triazine group such as the kind of side group on the ring and the leaving potential of the leaving group. Because of the nature of nucleophilic aromatic substitution, the reactivity of the triazine ring will be increased if the electron density on the ring is reduced. As a result, the rate of substitution reaction will be increased in the presence of an electron-withdrawing group or a leaving group with higher electronegativity.

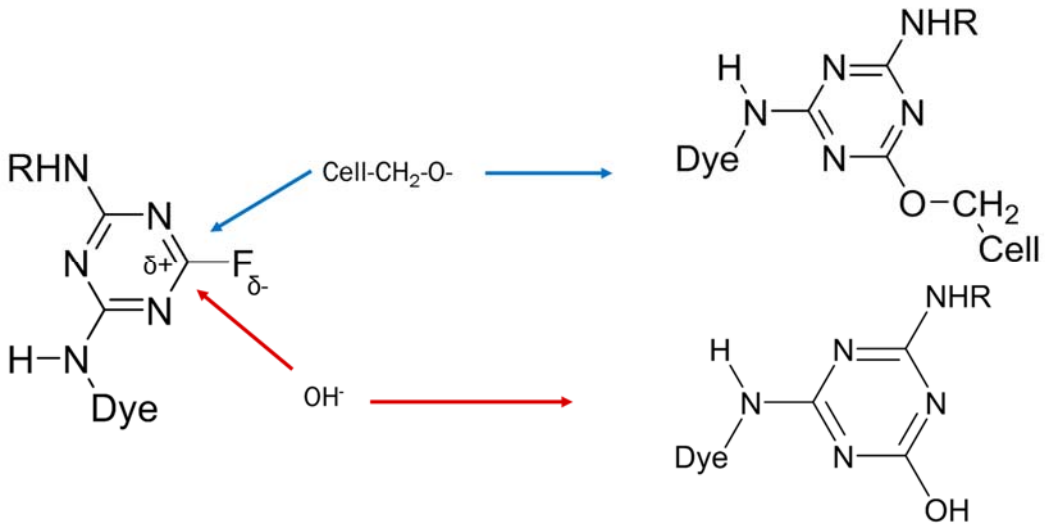

Figure 13 (a) Mechanism of nucleophilic substitution

In the nucleophilic addition, the sulfonate reactive group first go through an elimination of $NaHSO_3$ to become a reactive vinyl sulfone group due to the electron-withdrawing inductive effect of $-SO_2$. The α-carbon will have less electron density than the β-carbon, as a result, the α-carbon could be attacked by the cellulose anion and create a new covalent bond.

Cell = Cellulose, D = Chromophore

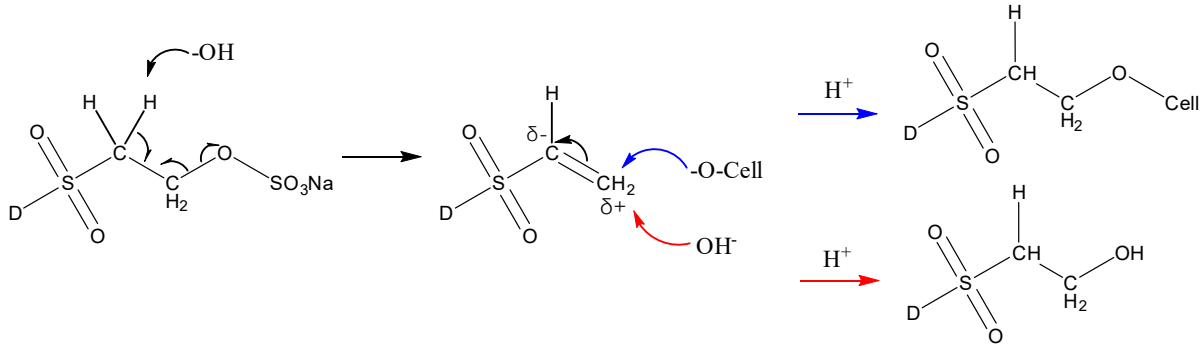

Figure 13 (b) Mechanism of nucleophilic addition

2.2.3. Hydrolysis of reactive dye

As the fixation reaction proceeds, the OH^- group from alkaline solution will act as a nucleophile and compete with cellulose anion to attack the reactive site on the dye. This would produce the hydrolysis form of the dye which will not only become a waste of material but also produce unstable color or "float color" on the fabric. To minimize the effect of hydrolysis during fixation, a kinetic mechanism of these two reactions was studied.*(23)*

$$R_F = k_F[D_F][CellO^-] \quad (6)$$

$$R_H = k_H[D_W][OH^-] \quad (7)$$

$$\frac{R_F}{R_H} = \frac{k_F}{k_H} \times \frac{[D_F]}{[D_W]} \times \frac{[CellO^-]}{[OH^-]} \quad (8)$$

These equations shows factors affecting the reaction rate of fixation and hydrolysis as well as the relative ratio between these them, where R represents the reaction rate, *k* represents the rate constant, D represents the concentration of reactive dye on the fabric and in dye bath, and $[CellO^-]$ represents the concentration of cellulose anion in the solution. As shown in equation (5), the reaction rate ratio between fixation and hydrolysis is made up of the ratio of the rate constant, the ratio of dye concentration between fabrics and solution and concentration ratio between cellulose anion and hydroxide. The first ratio is determined by Arrhenius equation which demonstrates the relationship between a certain reaction rate constant and its activation energy.*(24)* The second ratio is determined by the liquor bath of fixation process. The third ratio is determined by the pH of the solution. Studies have been found suggesting that by controlling the pH below 11 and liquor ratio around 1:30, the rate of fixation is 100 times higher than the hydrolysis reaction.*(22)*

Another successful way of increasing fixation rate is to design reactive dye with more than one reactive group. An example of this is the bifunctional reactive dyes Cibacron C developed by Ciba in the 1990s.*(25)* This kind of reactive dyes features the combination of monofluorotriazine reactive group and vinyl sulfone reactive group. As is shown in Figure 14 (a) and 14 (b)， due to the presence of two reactive groups, only when both of the reactive group gets hydrolyzed will the dye be deactivated so the dye will have a higher potential for fixation. The dye will still be able to react with cellulose even though one of the reactive groups has been hydrolyzed. Due to this special bifunctional reactivity, this kind of reactive dye is claimed to have a fixation rate near 95%.

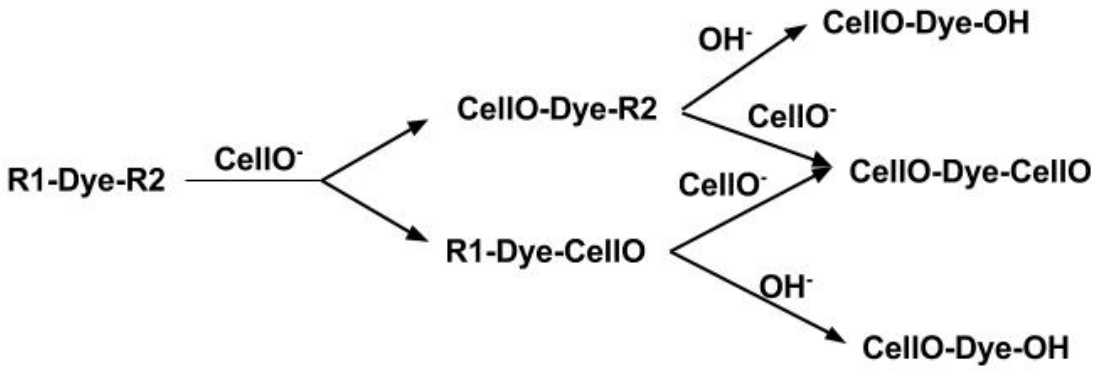

Figure 14 (a) Fixation bifunctional reactive dye

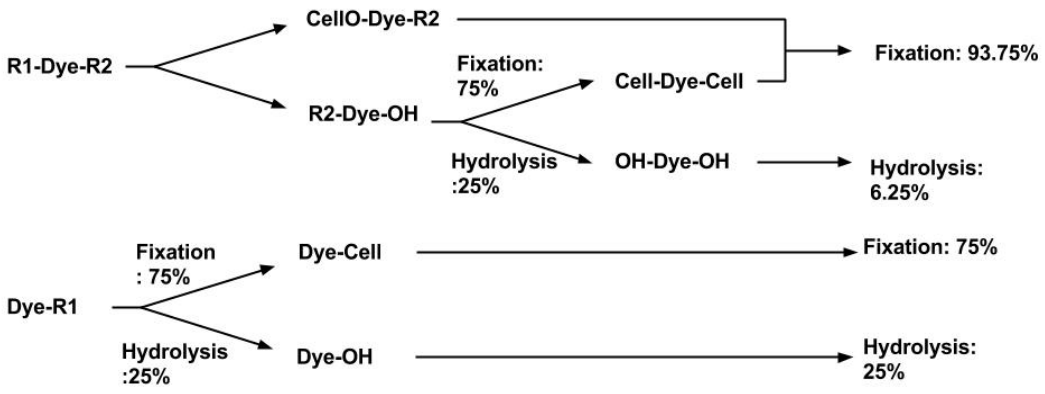

Figure 14 (b) comparison of Fixation properties between bifunctional reactive dye and monofunctional reactive dye *(25)*

2.3. Degradation of reactive dye fabrics

2.3.1. Chemical reactions on cellulose

Cellulose is a kind of semi-crystallized natural polymer made up by glucose unit in β-1, 4 linkages. As one of the most available natural polymers and the major component of cotton, the behavior of cellulose polymer chain plays an important role in the degradation of cotton fabrics.*(26)* A diagram of the chemical structure of cellulose is provided in Figure 15. The structure along the backbone of cellulose polymer shows two reactive sites available for reaction: the glycosidic bond between each glucose and other functional groups such as dye or flame retardant onto the chain of cellulose.*(3)*

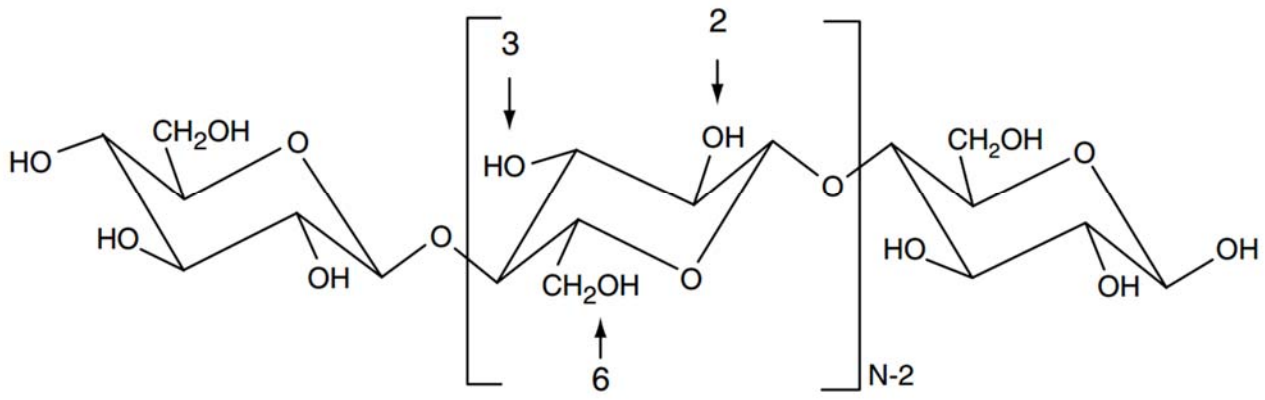

Figure 15 Chemical structure of cellulose

2.3.1.1. Effect of base treatment on cellulose

A series of wet processing processes such as desizing, sourcing, and mercerization involves treating cotton with base at different concentrations. In general, cellulose is very stable to an alkaline solution but if the fabrics were not cleaned thoroughly, the basic residue could serve as a catalyst for the oxidation by oxygen in the air. *(27)*

Cellulose under alkaline conditions undergoes a swelling process. Depending on the concentration of the base, the product from this process could be different. In a dilute solution (less than 9% sodium hydroxde), the swelling is reversible, but when the concentration exceeds 9%, the swelling become irreversible. Under this scenario the cotton fiber will shrink in the axial direction while it cross-section area gets expanded. After washing, the aggregation state of cellulose gets changed, which results in a decrease of the degree of crystallization from 70% to 50 % of the fiber. The bond force within the crystal region is also reduced which facilitates the penetration of liquid into the crystal region. Based on this phenomenon, a wet processing procedure called mercerization was developed by John Mercerin in 1844.*(3)* In this procedure,

bleached and sourced cotton fabric is treated with high concentrated sodium hydroxide (18-24%) before it is washed by water under applied strength to avoid the shrink of the fabric caused by irreversible swelling. Due to the decrease of the degree of crystallization, the fabrics' adsorption capability and reactivity get increased. Meanwhile, the mercerized cotton will have a better strength and dimensional stability than untreated fabrics.

2.3.1.2. Effect of acid on cellulose

Cellulose is very vulnerable to acid since the glycosidic bond that makes up its backbone could easily be hydrolyzed by acid under proper condition.*(28)* Figure 16 demonstrates the mechanism of this reaction. In this reaction, the hydrogen ion from acid serves as a catalyst which reduces the activation energy and speeds up the reaction. As the nature of the catalyst, the hydrogen ion will not be consumed during the reaction which means that in practice, after treatment with acid, the fabrics will have to be washed intensively in order to avoid the continuous damage caused by acid residue. In theory, when the reaction is finished, cellulose fiber will be completely hydrolyzed and the ultimate product will be glucose.

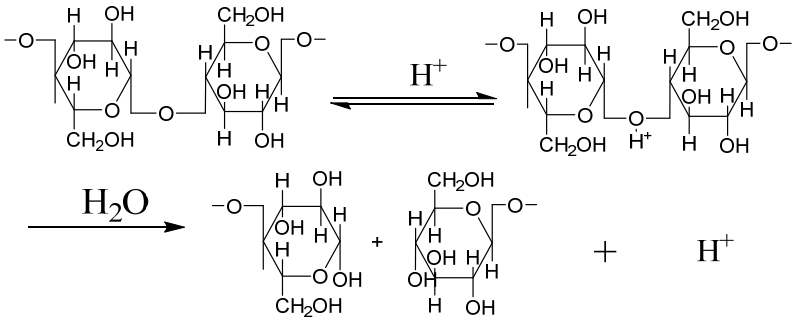

Figure 16 Acid hydrolysis of cellulose

Depending on the concentration of acid, the progress of this reaction will be different. In the case of highly concentrated acids such as sulfuric acid or hydrochloric acid, the reaction is homogeneous and the hydrolysis will proceed gradually and eventually produce glucose as ultimate product. In the case of dilute acid, the progress of reaction will depend on the region in contact. Initially, the acid will react rapidly with the amorphous region since aggregation structure in the region is less tight than crystalline region. After the amorphous region gets hydrolyzed, the acid starts to attack crystalline region and the reaction rate is significantly reduced as it becomes difficult for the acid to penetrate the tightly-assembled crystalline region.

3. Experimental

3.1. Materials

3.1.1. Solvents

ACS grade solvents such as methanol, acetonitrile, ethyl acetate, and 1-butanol were purchased from Sigma-Aldrich and used without any further purification. Distilled water was acquired from a Pure Lab Ultra water purification system from ELGA Lab Water. LC-MS Grade methanol and acetonitrile were purchased from VWR Analytical.

3.1.2. Dyes

The commercial reactive dye C.I. Reactive Yellow 174 was obtained from Cotton Incorporated. The structure of this bi-functional reactive dye was provided in Figure 17.

Reactive Yellow 174

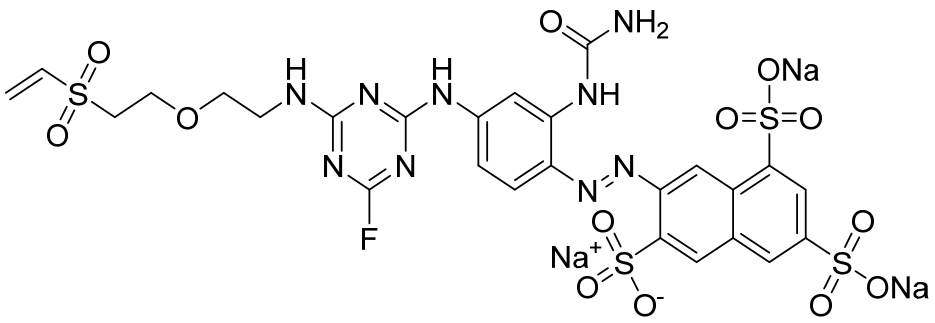

Chemical Formula: $C_{26}H_{23}FN_9Na_3O_{13}S_4$
Exact Mass: 884.9975

Figure 17 Structure of Reactive Yellow 174

3.1.3. Fabrics

White control fabrics and Reactive Yellow 174 dyed fabrics were provided by Cotton Incorporated. These single knit jersey clothes were made from 100% cotton. The fabrics were then bleached and dyed at the Dyeing and Finishing Application Laboratory at Cotton Inc.. Degraded fabrics (2 cm by 2 cm) were given by Cornell University. These fabrics were degraded for 45 and 90 days in the soil. Reactive Yellow 174 fabrics without degradation were cut into 2 cm by 2 cm square to match with the dimension of the degraded sample.

3.1.4. Chemicals

ACS grade sodium hydroxide powder, 30 % ammonium hydroxide solution, 1.0 M hydrochloric acid solution, 0.1M sulfuric acid solution, D-glucose powder and cellubiose powder were purchased from Sigma-Aldrich and used without further purification.

3.1.5. Other supplies

Aluminum TLC sheets, pH paper, disposable Luer-slip plastic syringes (1 mL), Millex-GV 13 mm, 0.22 μm polyvinylidene fluoride (PVDF) filters was purchased from Sigma-Aldrich. 15 x 45 mm, 1-dram glass vials were purchased from Fisher Scientific.

3.2. Wet Chemistry

3.2.1. Behavior of C.I. Reactive Yellow 174 under different pH condition

To establish a primary understanding the behavior of dye molecule under different pH conditions, a series of Reactive Yellow 174 solutions heated at different pH were prepared and analyzed by Time of Flight MS. First, the original pH of the commercial dye solution at 0.1M was measured by pH paper. Based on this native pH, two batches of dye solutions with pH of 3, 5, 7, 10, 12 were prepared by adding 0.05M sodium hydroxide solution or hydrochloric acid solution into the original dye solution. One batch of solution was heated on a Pierce Reacti-Therm^{TM} heating module at 80 ºC for 3 hours. Then solutions before and after the reaction were prepared for Thin Layer Chromatography (TLC) analysis to monitor the progress of reaction. After that, solutions after heating were diluted to a concentration of 100 μg per mL before analyzed by TOF MS. Figure 18 shows the photo of Reactive Yellow 174 solution heated at different pH.

Figure 18 Reactive Yellow 174 solution heated at different pH

3.2.2. Study on the Hydrolysis of Reactive Yellow 174 under alkaline condition

To investigate the reaction pathway of Reactive Yellow 174 hydrolysis under alkaline conditions, a series of hydrolysis reactions was designed. In order to investigate the effect of time and alkaline concentration on the progress of hydrolysis reaction, two groups of hydrolysis reactions were performed. The condition for these reactions were presented in Table 1. All the reactions in this section were performed in a 5-ml capped reaction vial and heated in a Corning hotplate. After the reaction, the vial was transferred into an ice bath and the reaction was quenched by adding 0.1 M hydrochloride acid to pH 7. Figure 19 showed the setup of experiment with different alkaline concentration.

Table 1 Conditions of hydrolysis reactions on dye solution

Group Number	Alkaline Concentration	Volume of alkaline solution	Volume of dye solution	Reaction time	Temperature
1	0.15%	1 ml	1 ml	5 minutes	60 ºC
1	0.15%	1 ml	1 ml	10 minutes	60 ºC
1	0.15%	1 ml	1 ml	20 minutes	60 ºC
1	0.15%	1 ml	1 ml	30 minutes	60 ºC
1	0.15%	1 ml	1 ml	60 minutes	60 ºC
1	0.15%	1 ml	1 ml	120 minutes	60 ºC
2	0.15%	1 ml	1 ml	2.5 hours	60 ºC
2	0.5%	1 ml	1 ml	2.5 hours	60 ºC
2	1.0%	1 ml	1 ml	2.5 hours	60 ºC

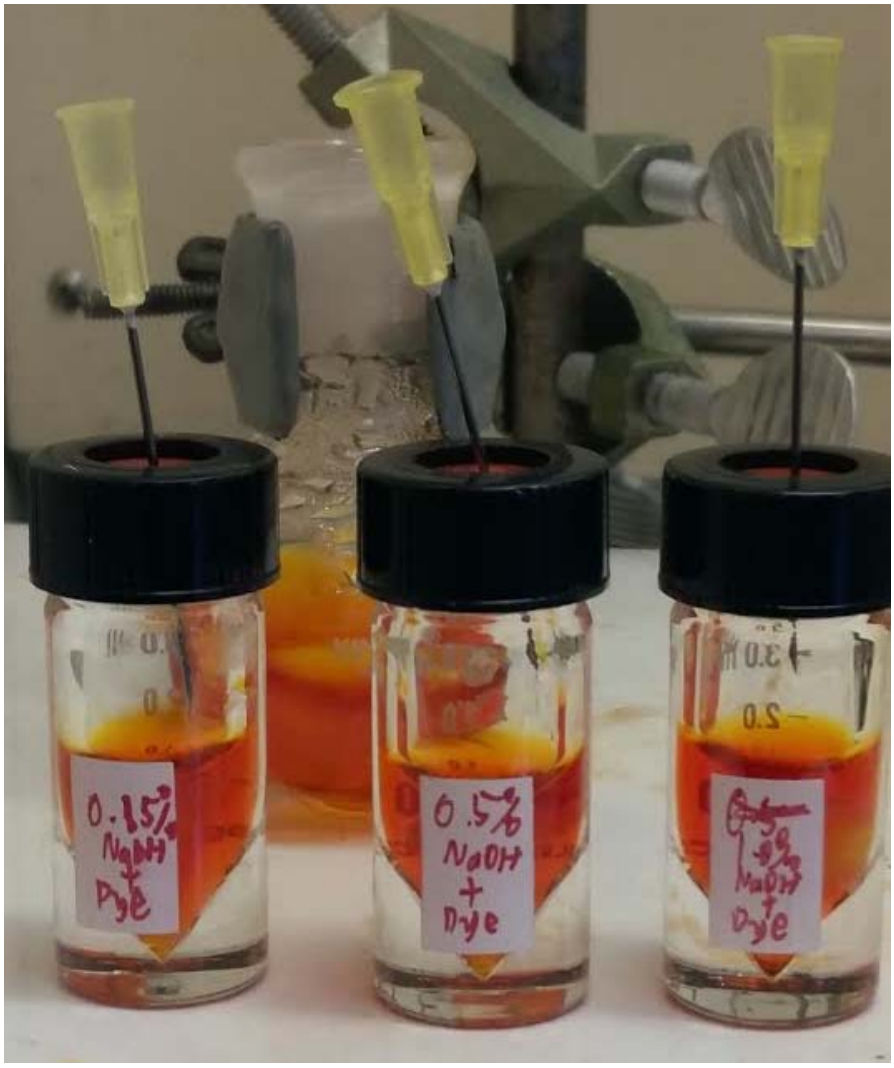

Figure 19 Experiment Setup of Reactive Yellow 174 alkaline hydrolysis at different concentration

3.2.3. Hydrolysis of Reactive Yellow 174 of colored fabrics

Due to the limited availability of degraded sample, a reliable method of extraction has to be developed before introducing the degraded samples. Preliminary experiments were carried out by treating undegraded Reactive Yellow 174 dyed fabrics with sulfuric acid and sodium hydroxide. The fabrics were cut into a 2 cm by 2 cm square piece to match the

dimension of degraded sample. To maximize the contact area of the fabrics, these 2 cm by 2 cm fabrics were cut into stripes and then into smaller fiber. These smaller fibers were added into a 5ml reaction vial with 2 ml of 0.1M sulfuric acid solution. The system was heated to 80 ºC on a Corning hotplate. The reaction was quenched by adding 0.05M sodium hydroxide into the solution to pH 7 in an ice bath. Then the solution was filtered by 0.22 μm polyvinylidene fluoride (PVDF) syringe filters to remove potential microfibers that may block the flow of HPLC. Meanwhile, another group of treatment on fabrics with distilled water was carried out as reference.

The treatments of not degraded fabrics with sodium hydroxide was carried out by using the same procedure of acid. But to investigate the influence of increased alkaline concentration on the progress of hydrolysis reaction, the treatment of not degraded fabrics with alkaline performed with three different concentration: 0.05%, 0.15%, and 1.5%. Figure 20 shows the setup of hydrolysis reaction on fabrics at alikiline condition.

Figure 20 Setup of acid treatment experiment on undegraded Reactive Yellow 174 fabrics

3.2.4. Thin-layer Chromatography

Thin-layer Chromatography (TLC) was applied to monitor the progress of synthesis reactions. The elution solvent used in this experiment was a mixture of ethyl acetate, methanol, acetonitrile, 1-butonal at a ratio of 1:4:2:1. The development of this solvent system was based

on existing studies and a series of empirical experiments.*(29, 30,)* The stationary phase used in this study is silica gel 60 F_{254}. The solution was spotted onto the surface of the sheet by 5-ul micro-capillary and dried in the oven for three minutes. Meanwhile, 2 ml of elution solvent was added into the TLC chamber and set for 5 minutes. Then the spotted TLC sheet or plated was placed into chamber and leaned on the bottle wall. When the elution is finished, the plate was taken out from the chamber and the R_f of each sample was calculated after the residue solvent evaporated. A Handheld UV light (Model ENF-260C) from Spectroline® was used to detect possible colorless components that subject to UV absorption.

3.3. Instrumental analysis

3.3.1. Spectrophotometric analysis

Spectrophotometric analysis was carried out to characterize the absorption properties of the degraded and undegraded Reactive Yellow 174 fabrics. The measurement of spectral reflectance of fabrics as well as their K/S value, an indicator of dye concentration developed by Kubelka and Munk in 1931*(31)*, were carried by using an X-rite Color i7 spectrophotometer and the following parameters: Specular inclusion, 10^o standard observer, small area view, D65 standard illuminant and 4 reading averaged. Because of the different surface texture of the fabrics, the measurement was performed twice on each side of the fabric and averaged.

Due to the limited quantity of degraded fabrics as well as its lack of structural integrity, the fabrics after degradation have to be modified to fit the standard measurement procedure of spectrophotometer. As a result, both of the degraded and undegraded fabrics were mounted with two 0.1 cm thick transparent glass slides. A photo of control undegraded fabrics and degraded fabrics was provided in Figure 21.

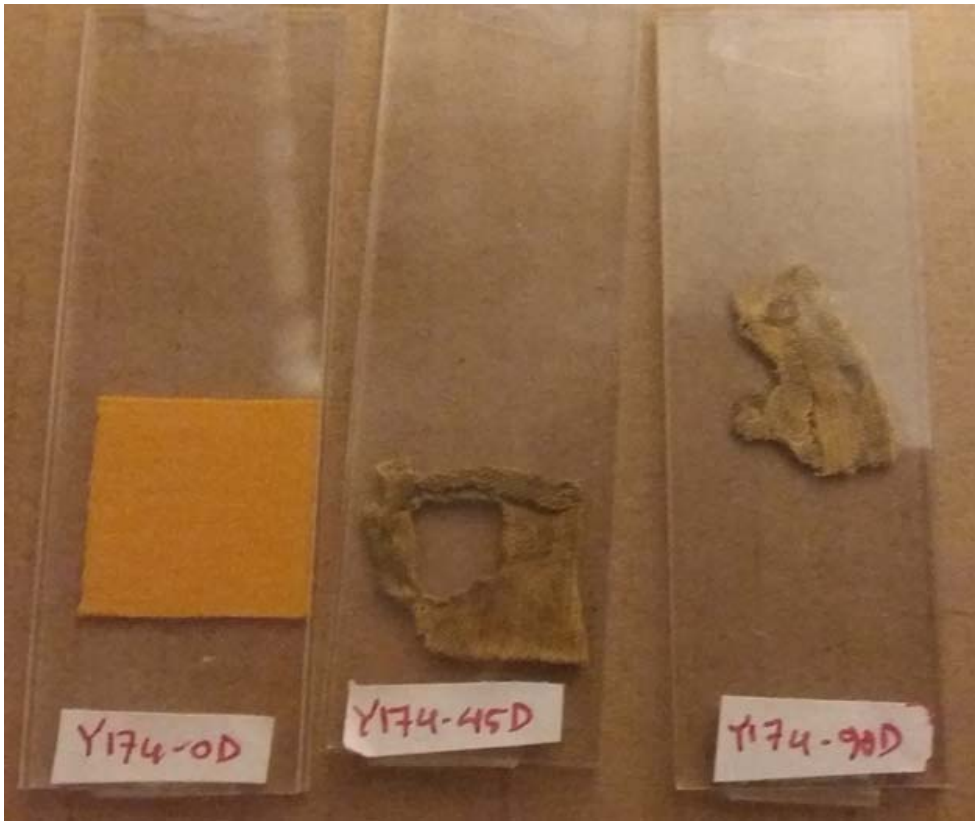

Figure 21 Photograph of degraded (45, 90 days) and not degraded R.Y 174 fabric

3.3.2. Analysis of the behavior of dye at different pH by TOF MS

To obtain a preliminary understanding on the behavior of Reactive Yellow 174 dye molecule under different pH conditions, TOF mass spectrometer analysis was conducted. Six solutions of 0.1M C.I. Reactive Yellow 174 after 3 hours of heating at 80 ºC were diluted with methanol to 100 µg per mL by mixing 10 µL of product solution was 990 µL methanol. Then the solution was introduced into MS via direct injection on a NE-300 syringe pump from New Era Pump System Inc. with the infusion rate set at 6uL per minute. Ionization was carried out in negative mode with the following parameters: gas temperature 350 ºC, drying gas 5 liters

per minute, nebulizer 50 psig, V_{cap} voltage 3500V. Time of flight mass analyzer was set with fragmentor voltage at 110 V, skimmer voltage 65 V, and OCT 1 RF V_{pp} at 750 voltage.

3.3.3. MS/MS study on the dissociation pathway of C.I. Reactive Yellow 174 and hydrolysis product

Tandem MS analysis was performed on C.I. reactive Yellow 174 dye molecule as well as its hydrolysis product was carried out to examine its dissociation pathways under Collision-Induced Dissociation (CID). The experiments were performed by targeted MS/MS acquisition function from Agilent MassHunter™ Acquisition interface. Native dye ions at m/z 419.5109 and hydrolysis product ions at m/z 418.5121, 416.5493 were selected as precursor ions which represents products from the hydrolysis reaction at different stage. These ions of interest were isolated using a narrow window (~1.3) and with Collision energy set at 15, as defined by MassHunter.

3.3.4. LC-MS Analysis

LC-MS analysis on the hydrolysis products from fabric and dye were performed on an Agilent Technologies 1260 High-Performance Liquid Chromatography (HPLC) system coupled to the Q-TOF mass spectrometer. Running solutions were prepared as follows: 10 µL of product solution was transferred to a 2-mL Agilent amber screw top glass LC vials (Part number: 5188-6535) and mixed with 990 µL of LC-MS grade methanol. The product solution from fabric treatment was transferred to the vial. The mobile phase was composed by an isocratic elution with water and acetonitrile at a ratio of 1:1 and an Agilent Poroshell™ 120 EC - C^{18}, 2.7 µm, and 3.0 x 100 mm reverse-phase column was used. The flow rate was set to 0.5 mL/min and total runtime for each sample is 5 minutes. Ionization was carried out in

negative mode with the following parameters: gas temperature 350 ºC, drying gas 5 liter per minute, nebulizer 50 psig, V_{cap} voltage 3500Vand fragmentor voltage at 175 V.

3.3.5. Potential volatile compound detection by GC/MS

GC-MS analysis of volatile compounds that may be originated from degradation process were perfomed on the mass spectrometry facility at the Chemistry Department at North Carolina State University. Degraded Reactive Yellow 174 fabrics and degraded control white fabrics were selected in this experiment. These fabrics were submerged into a washing solvent made up by acetonitrile and methanol at a ratio of 3:7 in a vial. The vial was shaken for one minute on a vortex mixer. Then the samples were transferred to the Chemistry department from GC-MS analysis. The instrument used was an Agilent 5975B GC/MS system with electron ionization and quadrupole mass analyzer. Regarding the setup in separation, the system phase consisted of two 30 cm columns filled with 5% Phenyl Methyl Siloxane with 250 um diameter as stationary phase and helium gas as mobile phase. A detailed report of GC/MS parameter was provided in Figure 22 (a) to (c).

```
------- -----------

Sample Inlet      :  GC
Injection Source  :  GC ALS
Mass Spectrometer :  Enabled


 No Sample Prep method has been assigned to this method.

================================================================================
                                6890 GC METHOD
================================================================================


OVEN
   Initial temp:  50 'C (On)                  Maximum temp:  325 'C
   Initial time:  3.00 min                    Equilibration time:  0.50 min
   Ramps:
      #  Rate  Final temp  Final time
      1 15.00       325        5.00
      2   0.0(Off)
   Post temp:  0 'C
   Post time:  0.00 min
   Run time:  26.33 min


FRONT INLET (SPLIT/SPLITLESS)              BACK INLET (SPLIT/SPLITLESS)
   Mode:  Splitless                           Mode:  Split
   Initial temp:  300 'C (On)                 Initial temp:  280 'C (On)
   Pressure:  7.61 psi (On)                   Pressure:  16.11 psi (On)
   Purge flow:  50.0 mL/min                   Split ratio:  50:1
   Purge time:  0.50 min                      Split flow:  73.4 mL/min
   Total flow:  53.7 mL/min                   Total flow:  77.5 mL/min
   Gas saver:  Off                            Gas saver:  Off
   Gas type:  Helium                          Gas type:  Helium


COLUMN 1                                   COLUMN 2
   Capillary Column                           Capillary Column
   Model Number:  Agilent 19091S-433          Model Number:  Agilent 19091S-433
   HP-5MS  5% Phenyl Methyl Siloxane          HP-5MS  5% Phenyl Methyl Siloxane
   Max temperature:  325 'C                   Max temperature:  325 'C
   Nominal length:  30.0 m                    Nominal length:  30.0 m
   Nominal diameter:  250.00 um               Nominal diameter:  250.00 um
   Nominal film thickness:  0.25 um           Nominal film thickness:  0.25 um
   Mode:  constant flow                       Mode:  constant pressure
   Initial flow:  1.0 mL/min                  Pressure:  16.11 psi
   Nominal init pressure:  7.62 psi           Nominal initial flow:  1.5 mL/min
   Average velocity:  36 cm/sec               Average velocity:  34 cm/sec
   Inlet:  Front Inlet                        Inlet:  Back Inlet
   Outlet:  MSD                               Outlet:  Front Detector
   Outlet pressure:  vacuum                   Outlet pressure:  ambient


FRONT DETECTOR (FID)                       BACK DETECTOR (NO DET)
   Temperature:  300 'C (On)
   Hydrogen flow:  40.0 mL/min (Off)
   Air flow:  450.0 mL/min (Off)
   Mode:  Constant makeup flow
   Makeup flow:  20.0 mL/min (On)
   Makeup Gas Type: Helium
   Flame:  Off
   Electrometer:  Off
```

Figure 22 (a) GC/MS instrument control parameters: page 1

```
SIGNAL 1
   Data rate:  20 Hz
   Type:  front detector
   Save Data:  Off
   Zero:  0.0 (Off)
   Range:  0
   Fast Peaks:  Off
   Attenuation:  0

SIGNAL 2
   Data rate:  20 Hz
   Type:  front detector
   Save Data:  Off
   Zero:  0.0 (Off)
   Range:  0
   Fast Peaks:  Off
   Attenuation:  0

COLUMN COMP 1
   Derive from front detector

COLUMN COMP 2
   Derive from front detector

THERMAL AUX 2
   Use:  MSD Transfer Line Heater
   Description:
   Initial temp:  280 'C (On)
   Initial time:  0.00 min
      #  Rate  Final temp  Final time
      1   0.0(Off)

AUX PRESSURE 3
   Description:
   Gas Type:  Helium
   Initial pressure:  0.00 psi (Off)

AUX PRESSURE 4
   Description:
   Gas Type:  Helium
   Initial pressure:  0.00 psi (Off)

AUX PRESSURE 5
   Description:
   Gas Type:  Helium
   Initial pressure:  0.00 psi (Off)

POST RUN
   Post Time: 0.00 min

TIME TABLE
   Time       Specifier                    Parameter & Setpoint


                              GC Injector

     Front Injector:
        Sample Washes                0
        Sample Pumps                 3
        Injection Volume          1.00 microliters
        Syringe Size               5.0 microliters
        PreInj Solvent A Washes      6
        PreInj Solvent B Washes      0
        PostInj Solvent A Washes     6
        PostInj Solvent B Washes     0
        Viscosity Delay              0 seconds
        Plunger Speed             Fast
        PreInjection Dwell        0.00 minutes
        PostInjection Dwell       0.00 minutes

     Back Injector:
No parameters specified

 Column 1 Inventory Number : HP001
 Column 2 Inventory Number : HP002

                            MS ACQUISITION PARAMETERS

General Information
```

Figure 22 (b) GC/MS instrument control parameters: page 2

```
------- -----------

Tune File               : atune.u
Acquistion Mode         : Scan


MS Information
-- -----------

Solvent Delay           : 4.00 min

EMV Mode                : Gain Factor
Gain Factor             : 1.00
Resulting EM Voltage    : 1482

[Scan Parameters]

Low Mass                : 45.0
High Mass               : 550.0
Threshold               : 150
Sample #                : 2       A/D Samples    4
Plot 2 low mass         : 50.0
Plot 2 high mass        : 550.0

[MSZones]

MS Source               : 230 C   maximum 250 C
MS Quad                 : 150 C   maximum 200 C

                          END OF MS ACQUISITION PARAMETERS

                           TUNE PARAMETERS for SN: US62744095
                         ----------------------------

 Trace Ion Detection is OFF.

 EMISSION    :      34.610
 ENERGY      :      69.922
 REPELLER    :      28.950
 IONFOCUS    :      80.667
 ENTRANCE_LE :      19.000
 EMVOLTS     :    1364.706
                              Actual EMV  :    1482.35
                              GAIN FACTOR :       1.02
 AMUGAIN     :    1541.000
 AMUOFFSET   :     122.813
 FILAMENT    :       2.000
 DCPOLARITY  :       0.000
 ENTLENSOFFS :      18.071
 MASSGAIN    :    -822.000
 MASSOFFSET  :     -37.000

                         END OF TUNE PARAMETERS
                       ---------------------------------


                           END OF INSTRUMENT CONTROL PARAMETERS
                           -----------------------------------
```

Figure 22 (c) GC/MS instrument control parameters: page 3

4. Results and Analysis

4.1. TLC on the behavior of dye under different pH

Result from TLC on the behavior of dye under different pH was shown in Figure 23. At room temperature, all the solution shows the presence of two separate spots at a nearly same height. These two spot has similar yellow color. So it is very likely that both of these two spots are related to the dye. Considering the separation principle of chromatography, the component with higher affinity to the stationary phase will travel at a lower speed, which results in a higher retention factor (R_f) The component with higher R_f will have higher polarity comparing with the with one with lower R_f. Combining these with the structure of C.I Reactive Yellow 174, we could expect these two spot could represent the hydrolyzed and unhydrolyzed form of the dye.

By comparing the TLC spots before and after hydrolysis, a qualitative understanding on the behavior this reactive dye under diffenrent pH conditions could be established. Figure 23 shows the TLCs results of the dye solutions of pH 3, 5, 6, 7, 10 and 12. It is noticeable that the color area showed in pH 10 was lighter than that in pH 5, 6 and 7, which indicated that the quantity of this component in pH 10 has been reduced after the reaction. Meanwhile, at pH 3 and pH 12, there was only one spot left after reaction and there is no present of the yellow area found in pH 5, 6, 7, and 10. This means that a considerable amount of starting material, which in this case is the native dye, has been converted into hydrolyzed dye that is more polar than the original form. Additionally, since pH also represents the concentration of hydroxide ion, based on the changes from pH 7 to pH 12, it is reasonable to claim that the hydrolysis of reactive Yellow 174 could be promoted by an increased concentration of sodium hydroxide.

Figure 23 TLC of Reactive Yellow at different pH before (left) and after heating (right)

4.2. Analysis of the hydrolysis reaction of Reactive Yellow 174 by Mass Spectrometry

4.2.1. TOF-MS spectra of Reactive Yellow 174 at different pH

MS spectrum of Reactive Yellow 174 solution at original pH (without additional acid or base) as well as background spectrum is provided in Figure 24 (a) to Figure 24 (c). As is shown in Figure 24 (a), a number of peaks with significantly high intensity can be observed. Among them, the peak of m/z 112.9867 is related to the methanol and water solvent. The peaks of 601.9784, 1033.9879, 1133.9684, and 1633.9494 in the background spectrum are identified as background peaks as they are related to the calibration matrix used to reduce the ppm error. Besides these background peaks, peaks of 272.0088 and 419.5077 were identified as triply and

doubly charged Reactive Yellow 174 by comparing the experimental m/z value and relative peak abundance and their isotopic distribution. Another noticeable sign found in Figure 24 (c) is the presence of peak at m/z 418.5089, which was identified as hydrolysis product at monofluorotriazine group (MFT) by checking the exacting the exact mass difference.

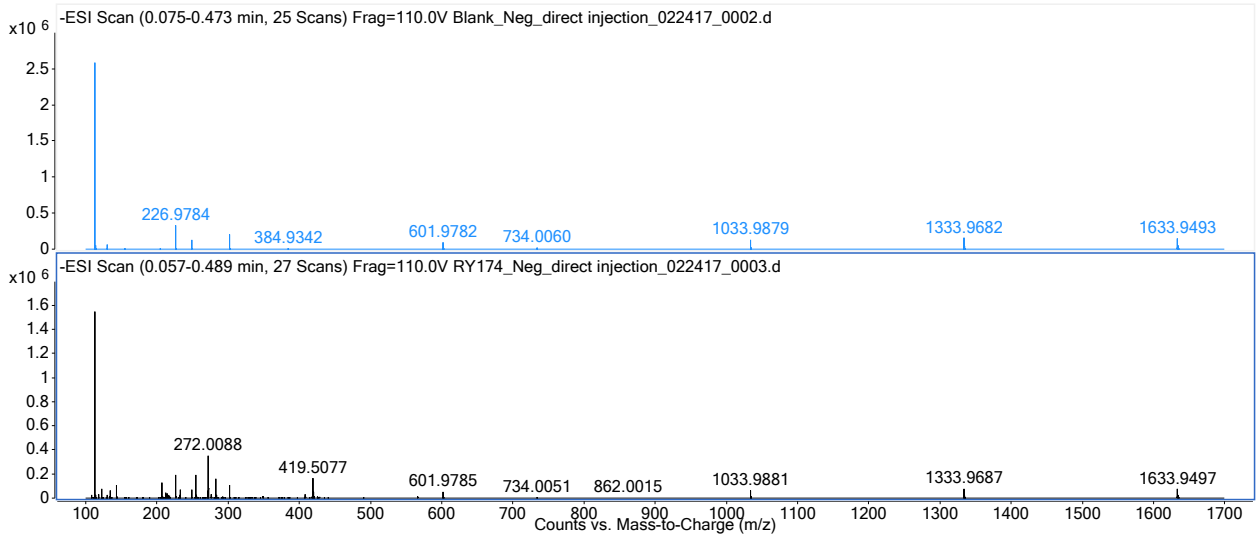

Figure 24 (a) Full spectrum of Reactive Yellow 174 solution heated at native pH

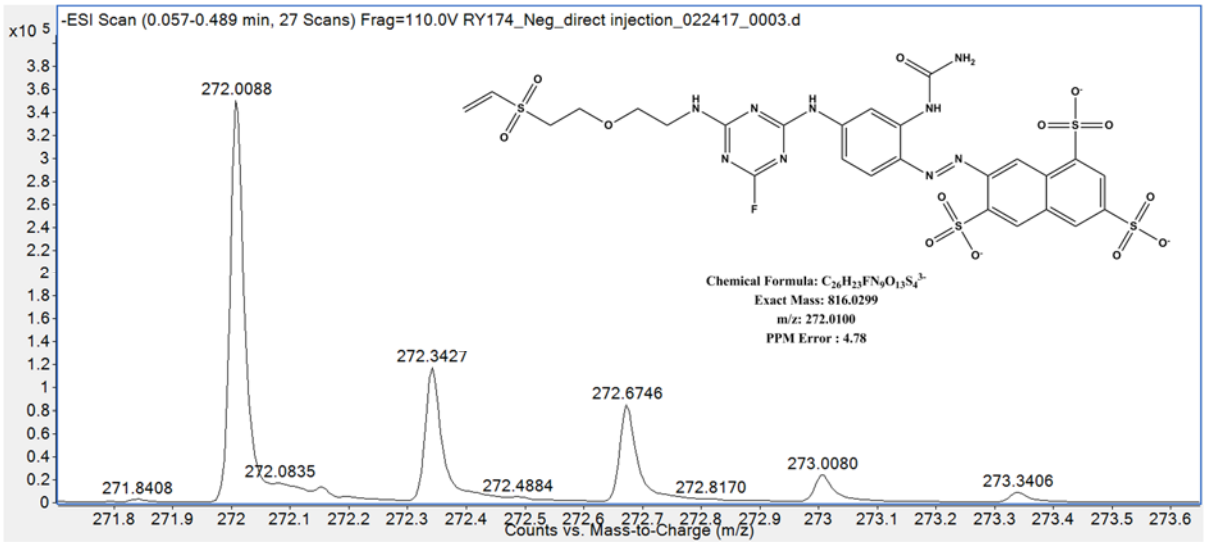

Figure 24 (b) Experimental isotropic distribution of triply charged Reactive Yellow 174

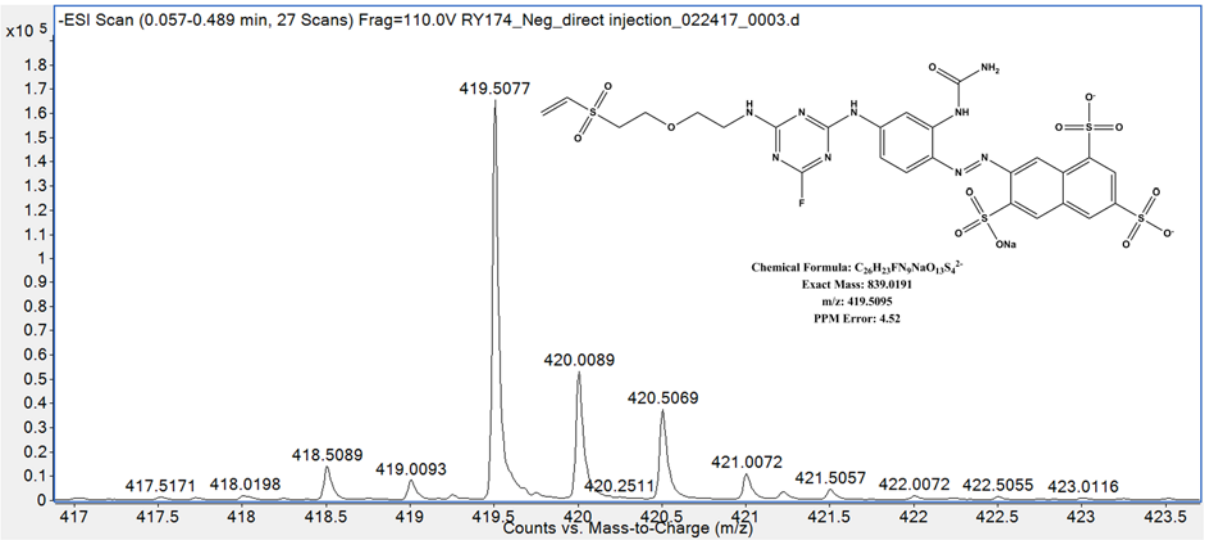

Figure 24 (c) Experimental isotropic distribution of doubly charged sodiated Reactive Yellow 174

Figure 25 (a) and (b) showed the MS spectra of the dye solution at pH 3 after 3 hours of heating at 80 ºC and the zoom in the spectrum of protonated and sodiated hydrolysis product at MFT group. One of the major change observed in Figure 25 (a) is that comparing with spectrum at native pH, the presence of peak around 419.5095 was no longer observed. Instead, two peaks at 407.5188 and 418.5097 were found, which were identified as protonated and sodiated hydrolyzed Reactive Yellow 174. By comparing those experimental m/z value with the theoretical exact mass, it is reasonable to claim that the hydrolysis product found in this solution is produced by hydrolyzing the monofluorotriazine group on the original dye. A confirmation of this structure by CID will be provided in the following section.

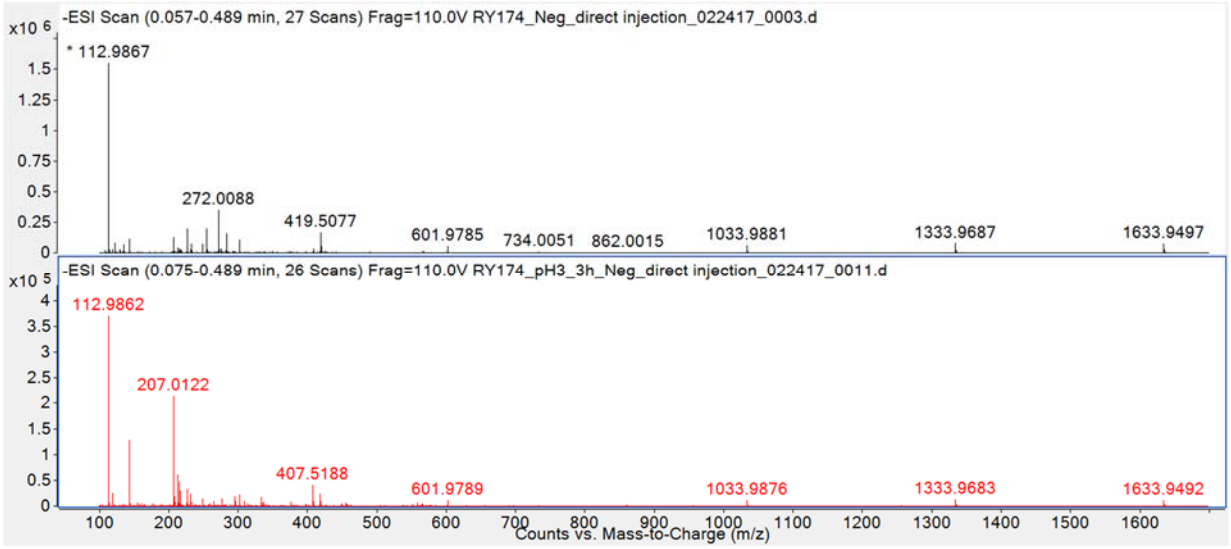

Figure 25 (a) Full spectrum of Reactive Yellow 174 solution heated at pH 3

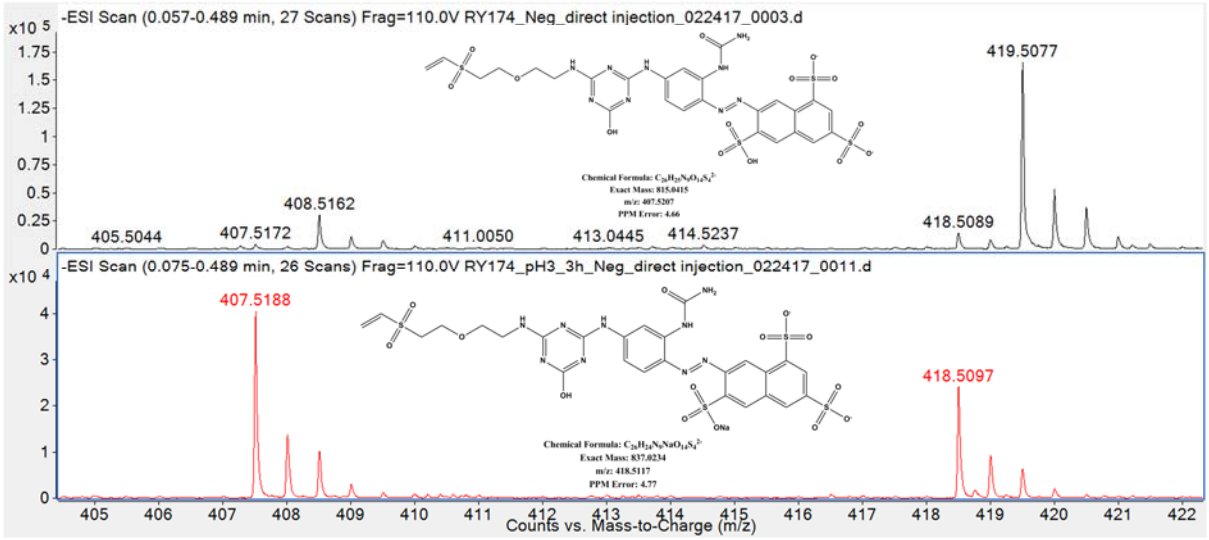

Figure 25 (b) Experimental spectrum of protonated and sodiated hydrolyzed dye in MFT group

Figure 26 and 27 shows the MS spectra of Reactive Yellow 174 solution at pH 6 and 7, respectively. Compared with spectrum at native pH, these two spectra did not show any significant changes in the distribution of peaks and behavior of the dye.

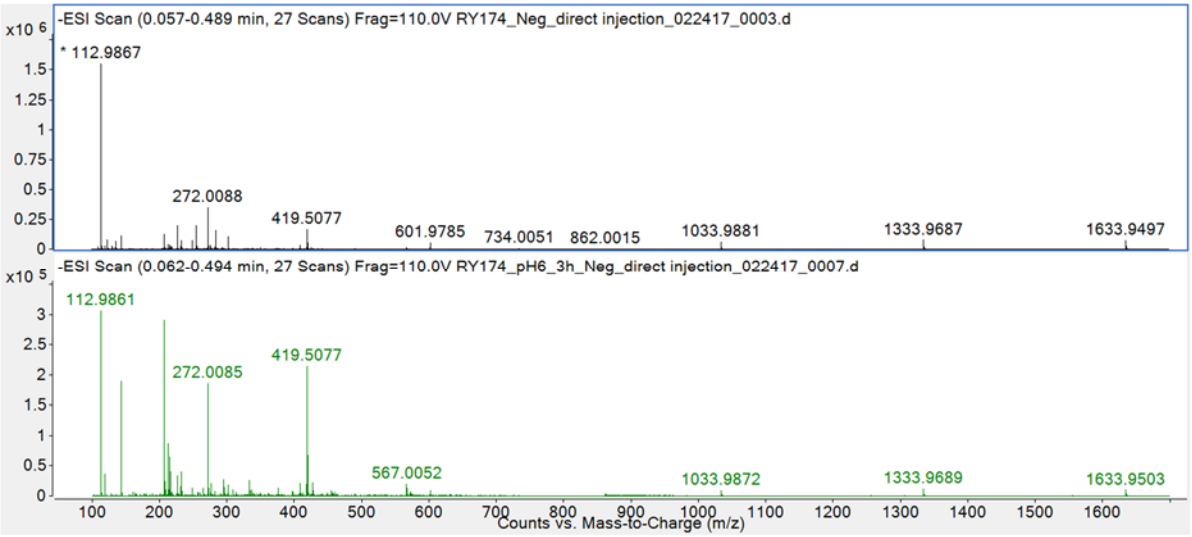

Figure 26 Full spectrum of Reactive Yellow 174 solution heated at pH 6

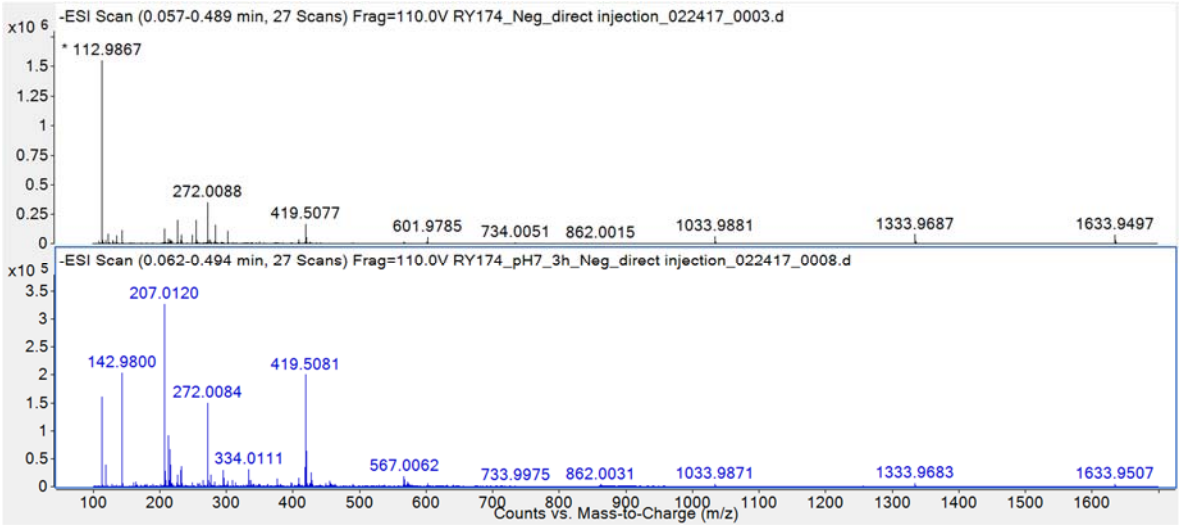

Figure 27 Full spectrum of Reactive Yellow 174 solution heated at pH 7

The full spectrum of dye solution heated solution at pH 10 was presented in Figure 28 (a). Compared with spectrum at native pH, the intensity of the peak at m/z 419.5095 was reduced while the peak at 418.5098 showed a significant increase in the intensity. A zoom in inspection in Figure 28 (b) shows an isotopic distribution interference around m/z 418.5098 and m/z 419.5082, which suggested that there was a mixture of hydrolysis product with the unreacted dye in the pH 10 solution. This merging of two isotropic distribution suggested that at this pH, after three hours of heating, the reaction condition was not strong enough to push the reaction to completion.

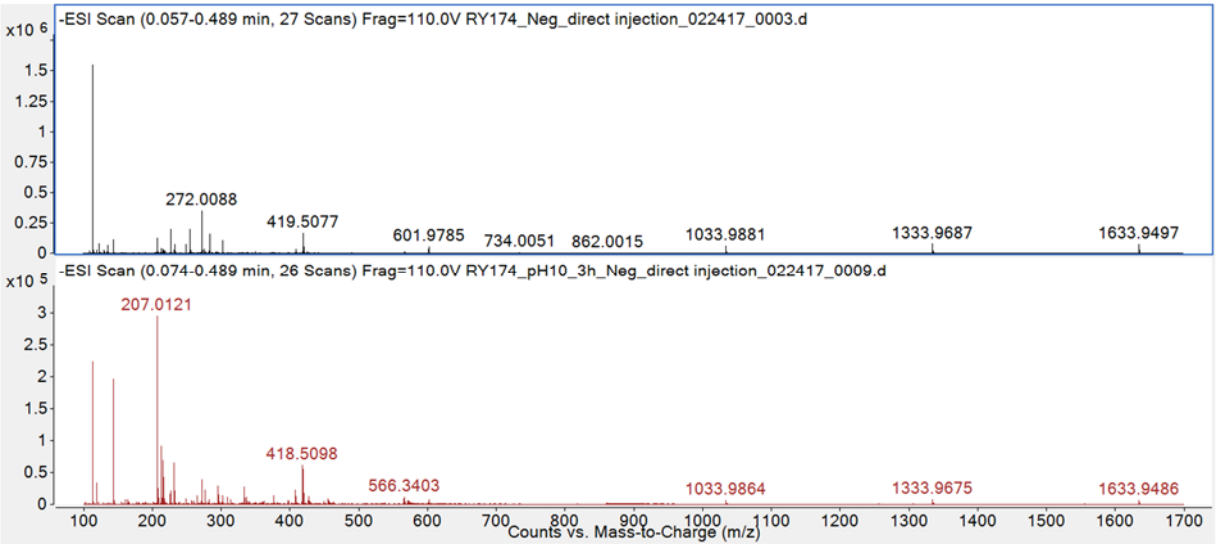

Figure 28 (a) Full spectrum of Reactive Yellow 174 solution heated at pH 10

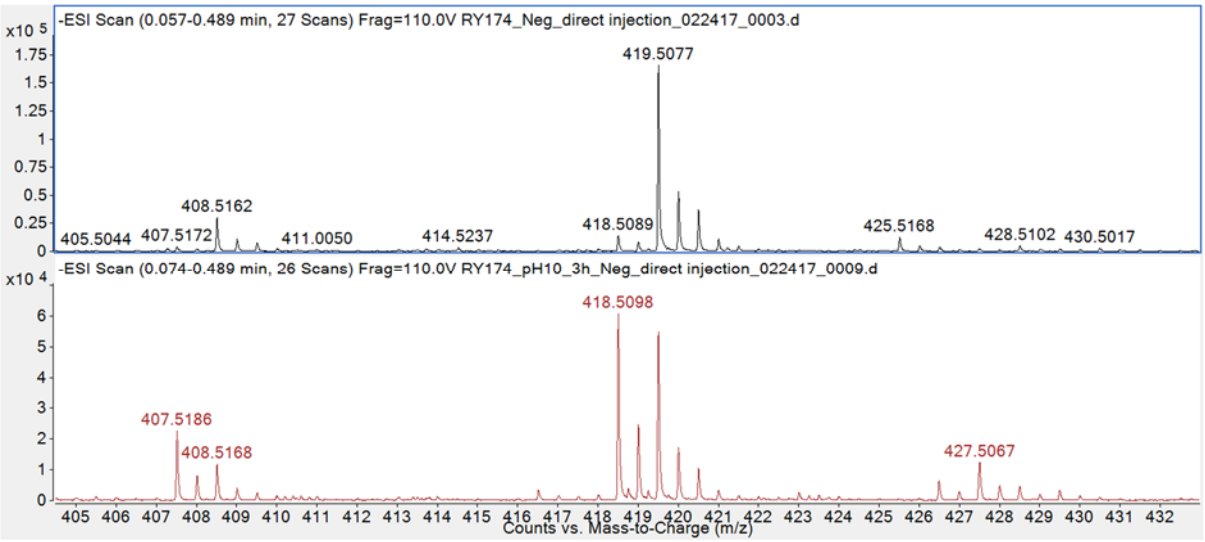

Figure 28(b) Zoom in spectrum showing the inference of isotropic distribution between m/z 407.5 and 419.5

Mass spectrum of pH 12 dye solution heated at 80 ºC for 3 hours is presented in Figure 30 (a). Compared with the mass spectrum from pH 3 solution, besides the peak of MFT hydrolysis product at m/z 407.5177 and 418.5096, there were two additional peaks at m/z 416.5232 and 427.5143 found in the spectrum. By examining the exact mass difference among these peaks, a correlation between them could be established where the peak at m/z 416.5232 and 427.5143 have 18 mass difference to the peak of 407.5177 and 418.5096. Considering the structure of this dye, it is expected that these two peaks could be identified as protonated and sodiated hydrolysis product in vinyl sulfone group and monofluorotriazine group. The structure of these two products is presented in Figure 29 (c) and (d). This presence of hydrolysis product peak and the near absence of native dye peak suggested that at pH 12, the high concentration of alkaline was able to considerably promote the progress of hydrolysis reaction. Another noticeable in Figure 29 (b) is that comparing with the spectrum from pH 12 solution,

which shows a considerable abundance of protonated hydrolysis product, shows a predominance in abundance of sodiated hydrolysis product. This could be explained by the difference in pH condition since the sodium ion from sodium hydroxide would dominate the population of positive ion in alkaline solution while the proton from hydrochloride acid would be the major positive ion in an acidic environment.

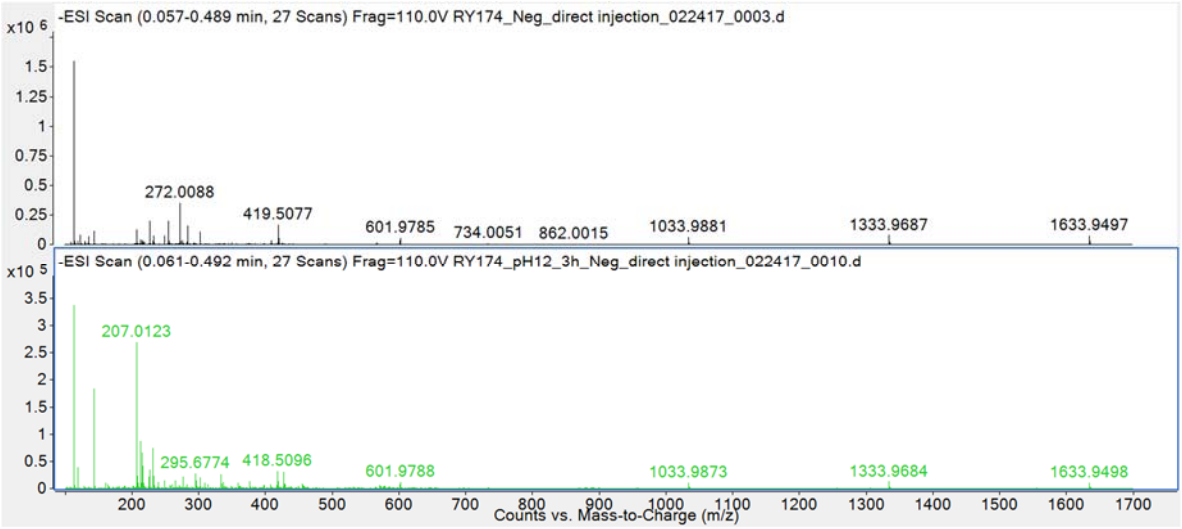

Figure 29 (a) Full spectrum of Reactive Yellow 174 solution heated at pH 12 featuring the absence of native dye

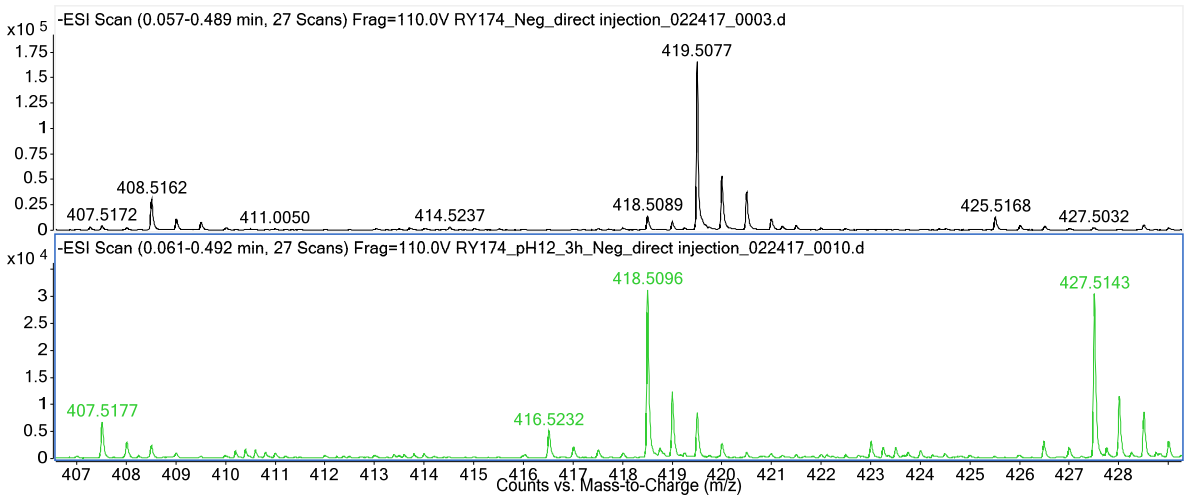

Figure 29 (b) Zoom in spectrum of protonated and sodiated Reactive Yellow 174 hydrolysis product in Vinyl Sulfone and Triazne group

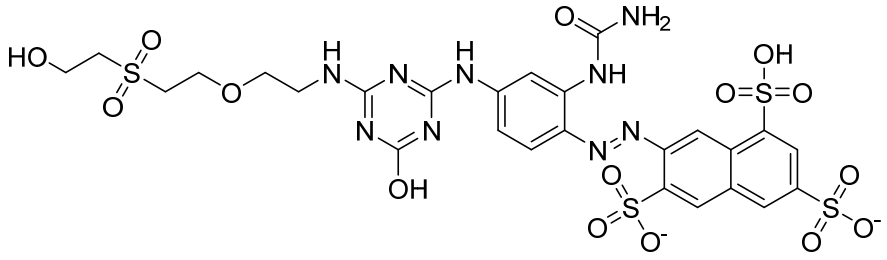

Chemical Formula: $C_{26}H_{27}N_9O_{15}S_4^{2-}$
Exact Mass: 833.0520
m/z: 416.5260 (100.0%)

Figure 29 (c) Structure of protonated hydrolysis product in Vinyl Sulfone and Monofluorotriazine group

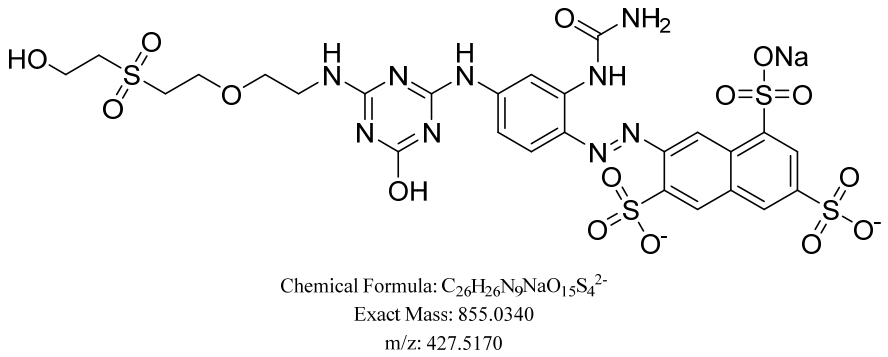

Figure 29 (d) Structure of sodiated hydrolysis product in Vinyl Sulfone and Monofluorotriazine group

4.2.2. MS/MS analysis on native dye and hydrolysis product

Doubly charged sodiated reactive Yellow 174 dye molecule at m/z 419.5109 was selected as precursor ion for MS/MS analysis. The MS/MS spectrum was presented in Figure 30 (a). At this fragmentation conditions, a series of fragments with m/z of 312.0117, 338.9996, and 351.9888 were observed. As shown in Figure 30 (a), the peak of m/z 351.9888 with a mass loss of 135.0416 was produced by removing the vinyl sulfone group as well as the ether group on the left part of the structure. The peak of m/z 338.996 and m/z 312.0117 were produced by losing additional C_2H_4 group and SO_3 group, respectively. By examining the exact mass difference between each of the product ions and precursor ion, the fragmentation pathway of unhydrolyzed Reactive Yellow 174 under CID could be established.

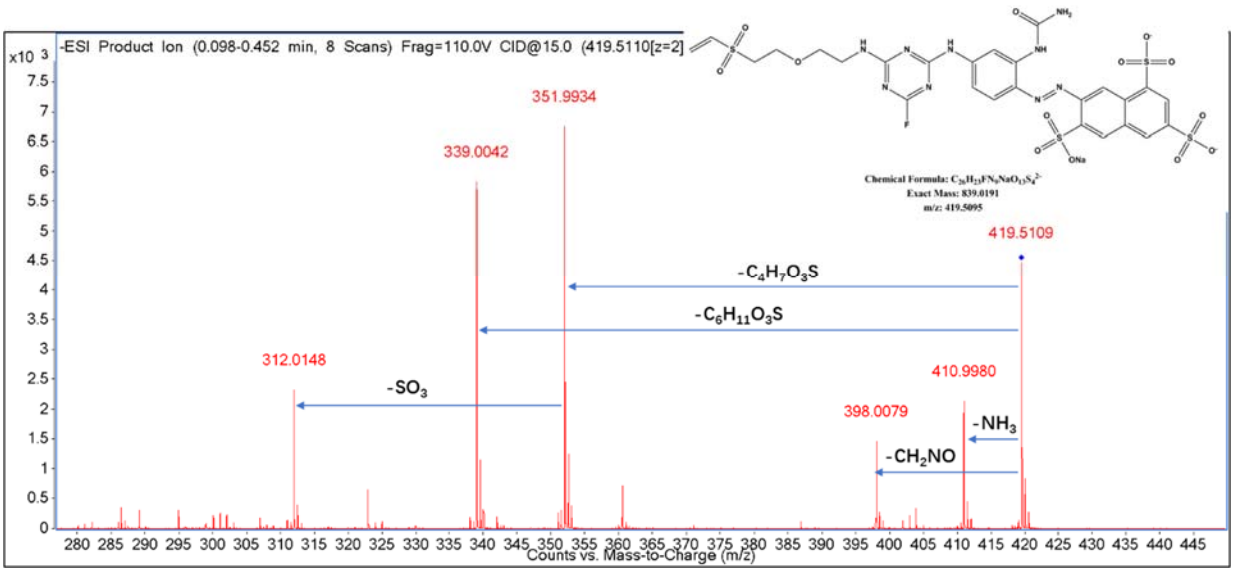

Figure 30 (a) MS/MS spectrum of doubly charged native Reactive Yellow 174

MS/MS spectra of sodiated Reactive Yellow 174 hydrolysis product in monofluorotriazine group from pH 12 and pH 3 were presented in Figure 30 (b). As is shown in the spectra, MS/MS spectra on m/z 418.5121 at pH 12 and pH 3 shared a same peak distribution. The most abundant peak at m/z 350.9915 and the peak at 338.0012 were due to the loss of vinyl sulfone group alone with the alkyl chain on left of the ether group. The next abundant fragment with a m/z of 409.9915, which corresponded to the loss of –OH group from the triazine ring. By examining the fragmentation pattern of Reactive Yellow 174 hydrolysis product, it proofs that the most vulnerable part in this dye is around the ether group since a majority of products are related to the breaking of this part.

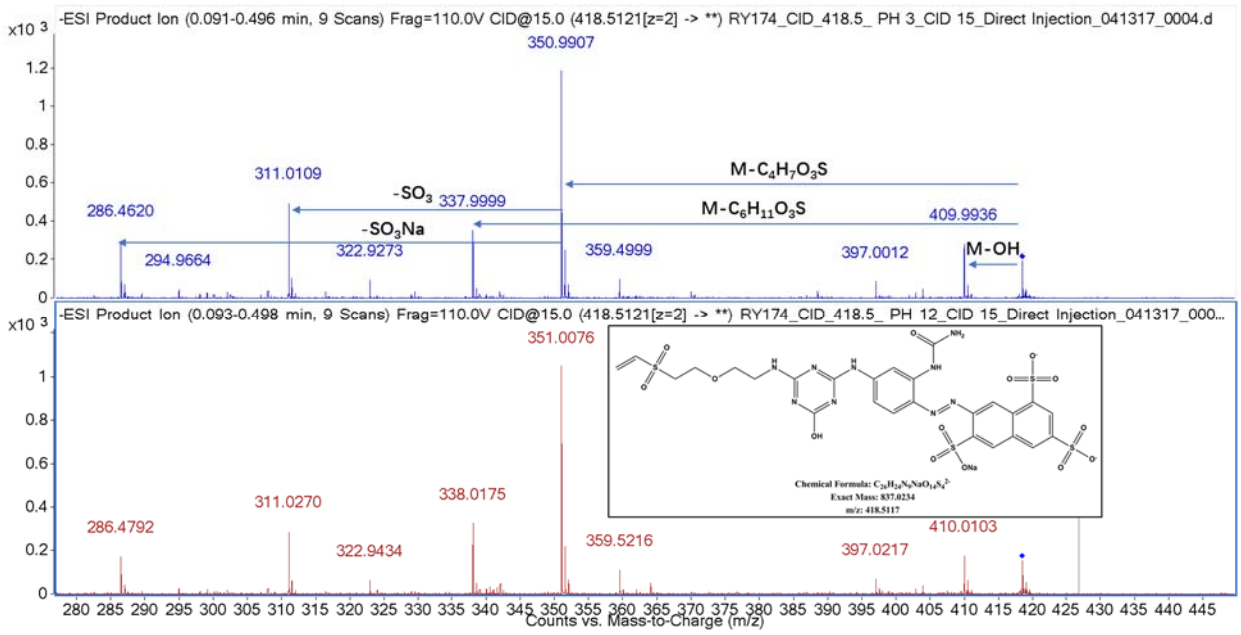

Figure 30 (b) MS/MS spectrum of doubly charged Reactive Yellow 174 hydrolysis product in monofluorotriazine group

MS/MS spectra on the peak of m/z 416.5553 from pH 12 solution was presented in Figure 30 (c). With collision energy at 15, a series fragment ions with m/z of 408.0093, 348.5124, 339.9987, and 327.0044 were observed. Among them, 408.0093 was produced by losing one OH group from the precursor ion while the peak of 348.5124 was produced by converting the ether group into a hydroxyl group with a loss of vinyl sulfone group. Based on this results, the product ions with m/z of 339.9987 and 327.0044 were generated by losing additional OH group and CH_2NO group, respectively. The structure of product ion with m/z 348.5124 is shown in Figure 30 (d)

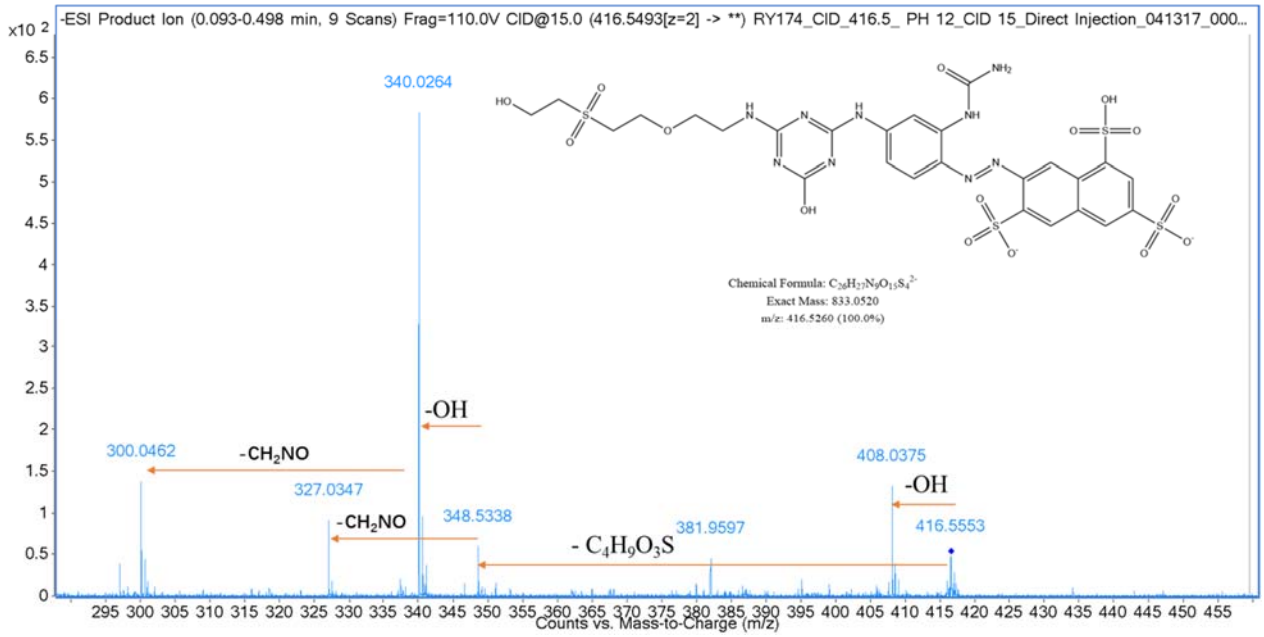

Figure 30 (c) MS/MS spectrum of doubly charged Reactive Yellow 174 hydrolysis product in Vinyl Sulfone and monofluorotriazine

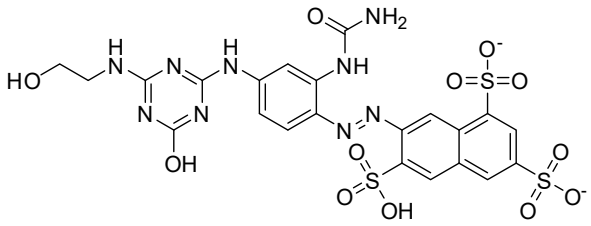

Chemical Formula: $C_{22}H_{19}N_9O_{12}S_3^{2-}$
Exact Mass: 697.0326
m/z: 348.5163

Figure 30 (d) Structure of fragment ion with m/z 348.5 showing the detachment of Vinyl Sulfone group

4.2.3. Reaction monitoring on hydrolysis of Reactive Yellow 174 by LC-MS

Figure 31 (a) showed a series of DAD chromatograms obtained from the alkaline hydrolysis of Reactive Yellow 174 at different time stages. The detection wavelength was set

at 430 nm. By checking the change in retention time, it is observed that as the reaction proceeds over time, the original dye peak was converted into something with higher polarity. This conversion of polarity reached completion after 30 minutes of reaction, the reaction was able to convert the native dye molecule into a different form with higher polarity. The detail composition of each system will be examined by comparing the MS spectra.

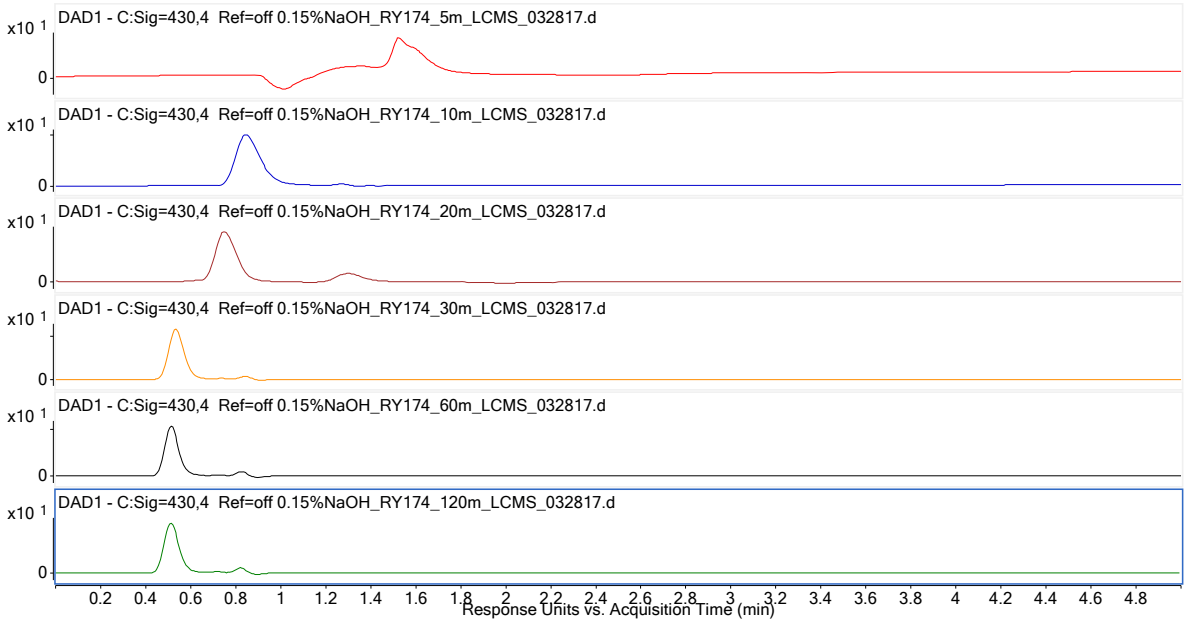

Figure 31 (a) DAD chromatogram of hydrolysis of reactive Yellow 174 dye at different time

Additionally, the LC-MS spectra corresponding with the DAD chromatogram of the reaction at different times was extracted and presented in Figure 31 (b). In these spectra, a series of peaks representing the products from different stages of the reactions were found. For instance, the peak at m/z 408.5238 represents the unreacted dye, the peak of 407.5265 represents the hydrolysis product in monofluorotriazine group, and the peak of m/z 416.5538 represents the hydrolysis product in vinyl sulfone and monofluorotriazine group. Since all six of the spectra were gathered using the same condition, the change in the peak abundance ratio

over time could also be interpreted as the progress of hydrolysis reaction over time. At the starting stage of the reaction, specifically, from 5 to 10 minutes, there was a predominance of m/z 408.5238 peak and a 407.5265 peak that is almost one-fifth of the 408.5238 peak. This suggest that there was already some single hydrolysis product in the starting material.

As the reaction time reaches 20 minutes, the peak abundance of m/z 407.5485 and 416.55538 increased while the peak abundance of m/z 408.5238 was reducing. These results suggested that after 20 minutes of reaction, a considerable amount of starting material was converted into the hydrolysis product through nucleophilic substitution on monofluorotriazine (MFT) group. By comparing the level of increasing in peak abundance of m/z 407.5485 to the same of 416.5538, it is reasonable to speculate that the generation of singly hydrolyzed product is easier than the generation of doubly hydrolyzed product. Then at 30 minutes, although the peak of m/z 408.5 still had a noticeable abundance, it was believed that most of the starting material had been converted into the hydrolysis product since the interfering of isotropic distribution between the peak of m/z 407.5485 and 408.5489 found in 20-minute spectrum has disappeared. As the reaction reached 60 minutes and then 120 minutes, it was observed that the peak of m/z 407.5322 was reduced and the peak of m/z 416.5538 got increased. This suggested that at the beginning of hydrolysis reaction, the native dye would be hydrolyzed at monofluorotriazine group through nucleophilic substitution. Then at 120 minutes, these single hydrolysis product gets hydrolyzed at the vinyl sulfone group via nucleophilic addition.

Another noticeable peak which was not shown in Figure 31 (b) is the peak of m/z 348.5538, which was identified as the degradation product of the dye. A table summarizing the abundance of the peaks discussed above is presented in Table 2.

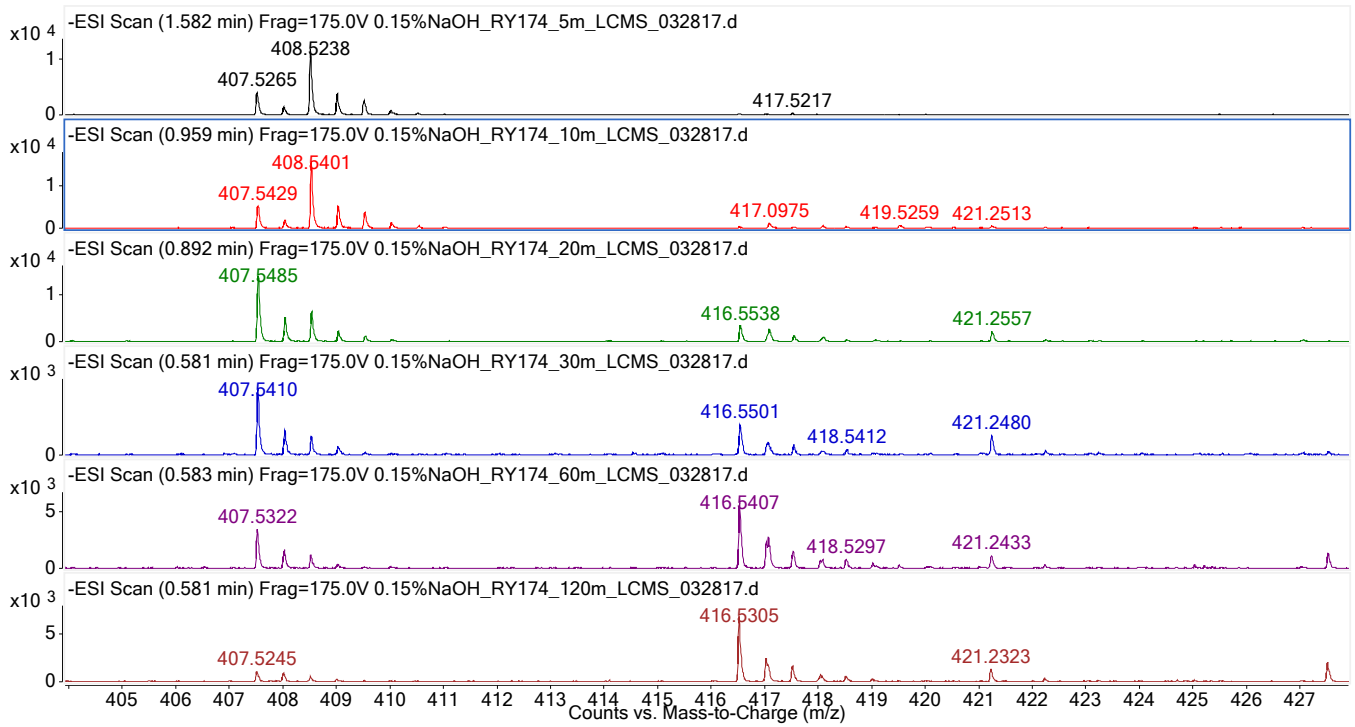

Figure 31 (b) LC-MS spectra on Hydrolysis of Reactive Yellow 174 at different time

Table 2 Peak Abundance of the hydrolysis products at different condition

Mass to charge ratio	407.5485	408.5489	416.5538	348.5273
Condition	Abundance			
60 ºC, 5 min, 0.15% NaOH	4061.12	11985.1	184.1	N/A
60 ºC, 10 min, 0.15% NaOH	5214.00	15689.98	N/A	N/A
60 ºC, 20 min, 0.15% NaOH	14024.82	6489.75	3390.39	868.08
60 ºC, 30 min, 0.15% NaOH	4287.97	1223.46	1970.74	247.27
60 ºC, 60 min, 0.15% NaOH	3340.89	1202.53	5807.36	799.35
60 ºC, 120 min, 0.15% NaOH	1036.97	566.74	6952.97	1315.01
60 ºC, 2.5 hours, 0.15% NaOH	610.53	322.75	3268.53	1326.1
60 ºC, 2.5 hours, 0.5% NaOH	655.79	403.35	3060.91	5299.64
60 ºC, 2.5 hours, 1.0% NaOH	N/A	N/A	986.52	7680.26

To verify the influence of alkaline concentration on the progress of reaction. Another group of spectra obtained from reactions with different concentrations of sodium hydroxide was presented in Figure 31 (c) and the peak abundance of native and hydrolysis product was enlisted in Table 1. As is shown in these spectra, in reaction with 0.15% NaOH, the peak of m/z 407.5445 was detected and the peak abundance of m/z 348.5376 is lower than that of 416.5491. This suggests that at this concentration, most of the native dye have been converted into the hydrolysis product. As the concentration of sodium hydroxide increases, the peak abundance ratio between m/z 348.5376 and m/z 416.5491 increases. This suggests that although the increasing alkaline concentration would push the reaction to completion, it also promotes the degradation of the dye. Additionally, this means that to preserve the structural integrity of the dye, the concentration of alkaline needs to be controlled at a certain level.

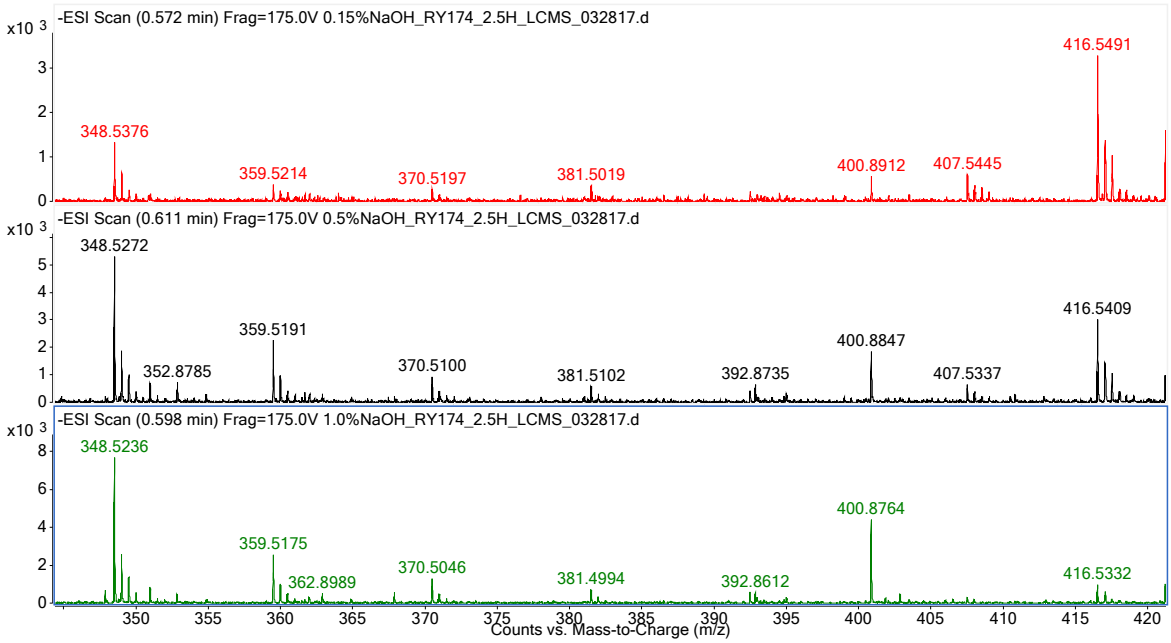

Figure 31 (c) LC-MS spectra on Hydrolysis of Reactive Yellow 174 with different alkaline concentration

4.2.4. LC-MS Study on the Hydrolysis of undegraded Reactive Yellow 174 fabrics

In order to study the behavior of the fabrics under different pH conditions, DAD chromatograms were obtained from the hydrolysis of undegraded fabrics at different pH conditions (Figure 32 (a)). As is shown in these chromatograms, both of the acid and the alkaline were able to remove a certain amount of colorant from the fabrics, but considering the area of DAD peak, the alkaline conditions were able to remove more dye from the fabrics.

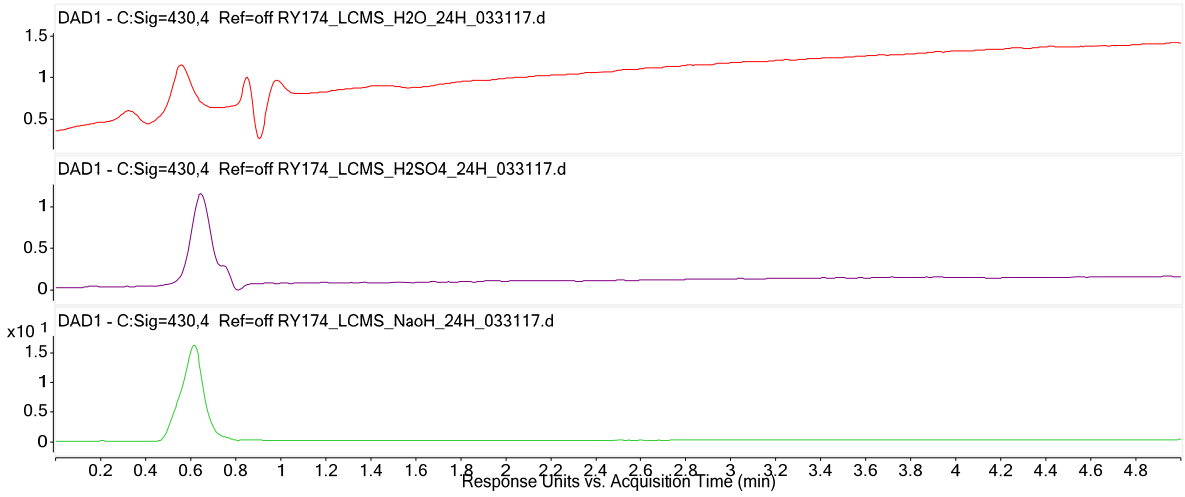

Figure 32 (a) DAD Chromatogram on the hydrolysis of Reactive Yellow 174 fabric at different pH condition

The MS spectra extracted from the DAD chromatogram are shown in Figure 23 (b). Basic hydrolysis showed a peak of m/z 179.0439, which represents the deprotonated glucose, and a peak with m/z 348.4919 representing the degraded reaction product of the hydrolysis product. These spectra in Figure 23 (b) suggests that sodium hydroxide is able to hydrolyze the reactive dye on the fabrics but also results in a degradation of dye on vinyl sulfone group.

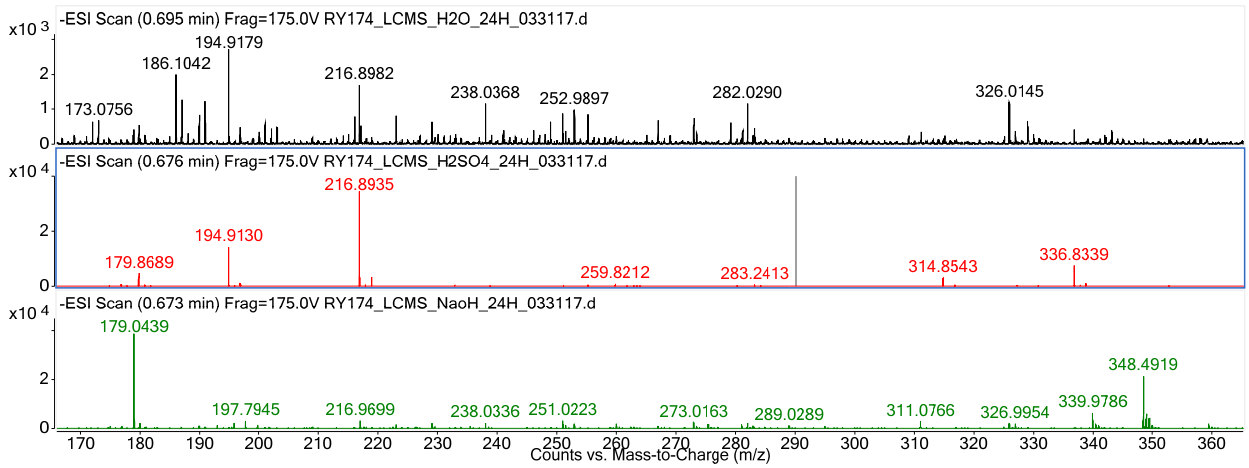

Figure 32 (b) LC-MS on the hydrolysis of Reactive Yellow at different pH condition

To verify the influence of sodium hydroxide concentration in this process, another set of reactions was carried out with increased alkaline concentration. As is shown in Figure 32 (c), as the sodium hydroxide concentration increases, the ratio between peak m/z 348.5175 and m/z 416.5286 increases dramatically. This suggests that an increased concentration of sodium hydroxide would hydrolyze the dye on the fabrics and promote the degradation of dye.

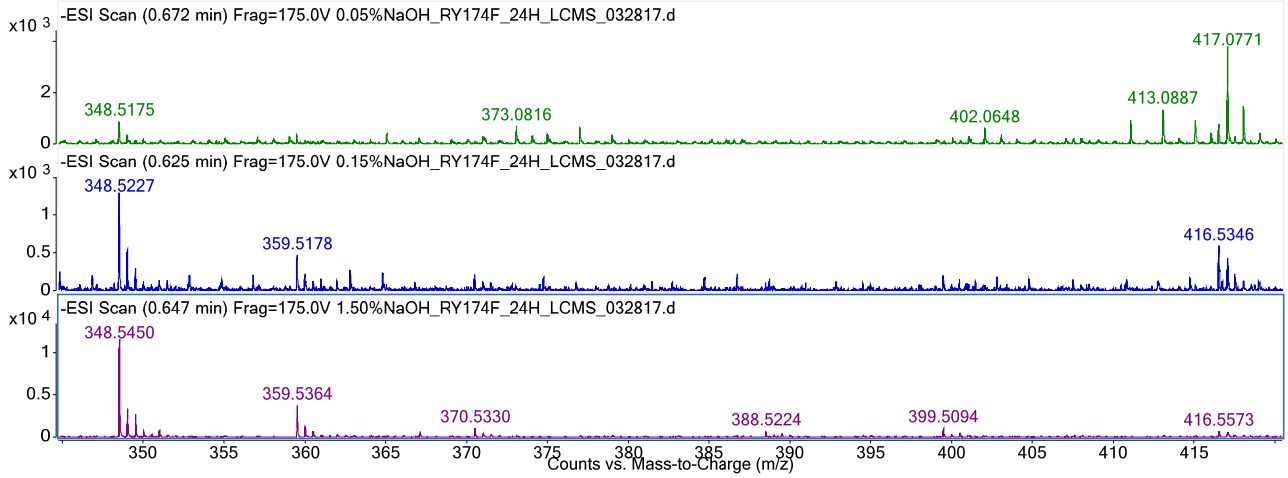

Figure 32 (c) LC-MS on the alkaline hydrolysis of Reactive Yellow at different concentration

4.3. Characterization of degraded fabrics

4.3.1. Spectral properties of Reactive Yellow 174 Fabrics with and without degradation

The absorption curve of Reactive Yellow 174 colored fabrics before and after the degradation was presented in Figure 33. It is expected that the λ_{max} of the undegraded fabrics will be around 440 nm. With this in mind, it will be expected that for degraded fabrics the λ_{max} absorption will decrese due to the change of dye concentration on the fabrics. This suggests that there is a noticeable amount of dye lost during the degradation which caused a decrease in dye concentration on the fabrics. Additionally, this figure indicates that even after 90 days of degradation, there is still a considerable amount of intact dye on the fabrics, which means that if the degraded fabrics were treated in the same condition as the fabrics without degradation, the results will show a certain level of similarity.

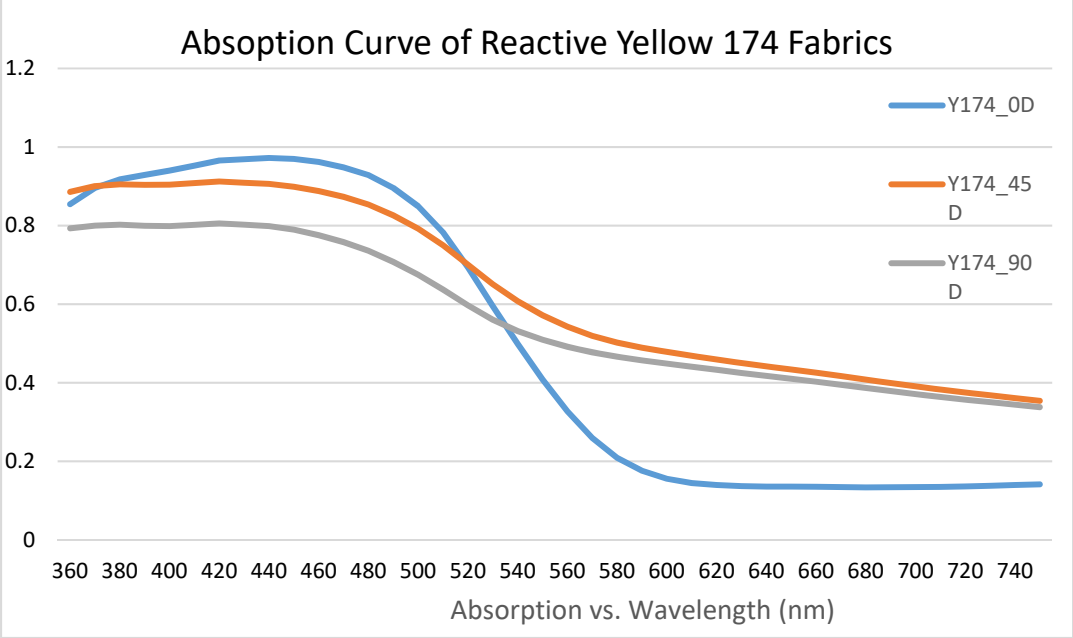

Figure 33 Absorption Curve before and after the Degradation

4.3.2. GC-MS spectra on degraded fabrics extraction

GC-MS is usually used to detect volatile compounds in a certain mixture.*(12)* Modern GC-MS are often equipped with library search program to generate a match based on a collection of EI spectra. The purpose of this GC-MS study to extract and detect possible generation of volatile compounds due to degradation of dye. The chromatogram of degraded white control fabrics washing liquid was presented in Figure 34 (a). As is shown in this chromatogram, most of the peaks with significant abundance are located within a retention time range of 14 to 17 minutes. A high abundance peak can be observed at 22.8 minutes.

A closer examination at 14 to 17 minutes showed that among all the peak in this region, peaks at 15.236, 15.464, and 16.519 minutes showed even higher abundance than others. The MS spectra of these three peaks were presented in Figure 34 (b) to Figure 34 (d). According to the report of MS system, with match quality of nearly 99 percent, they were identified as hexadecanoic acid-methyl ester, n-Hexadecanoic acid, and Octadecanoic acid - methyl ester, respectively. All of these three compounds could be classified as fatty acid or fatty acid ester. The most common use of fatty acids and fatty acid esters in the textile industry to serve as surfactants in detergents or wetting agents. Regarding the peak at 22.853 minutes which is shown in Figure 34 (e), it is identified as γ-Sitosterol, which a kind of cholesterol commonly was found in plants.

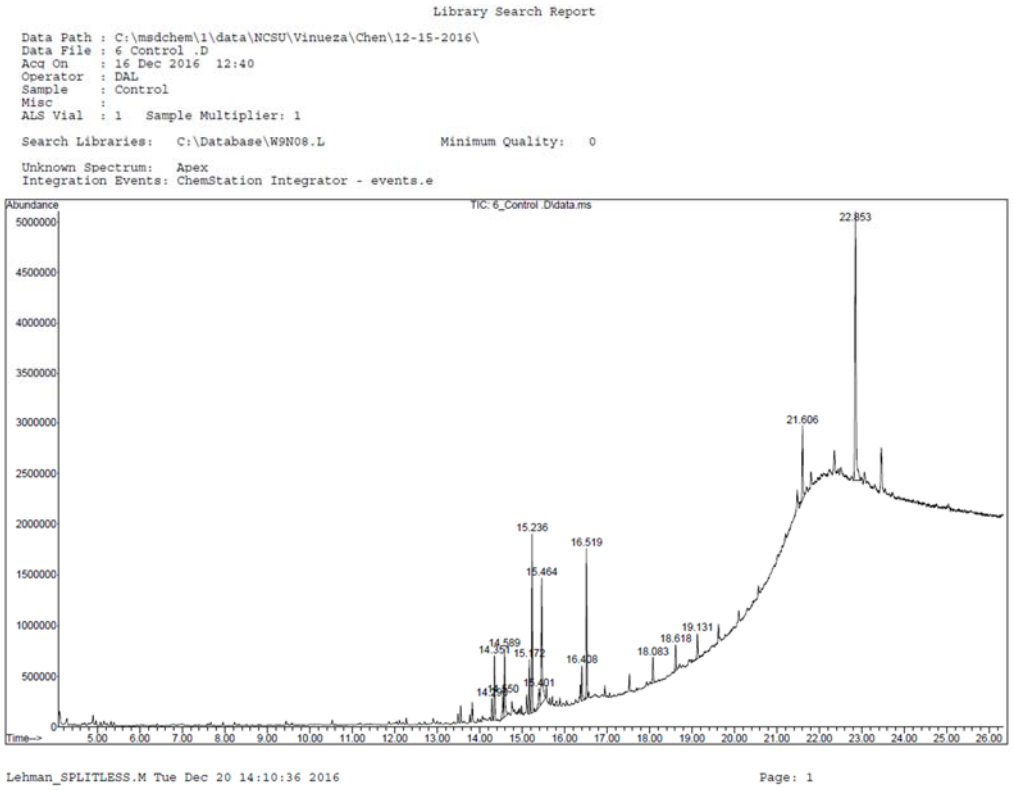

Figure 34 (a) GC Chromatogram of degraded white fabrics washing liquid

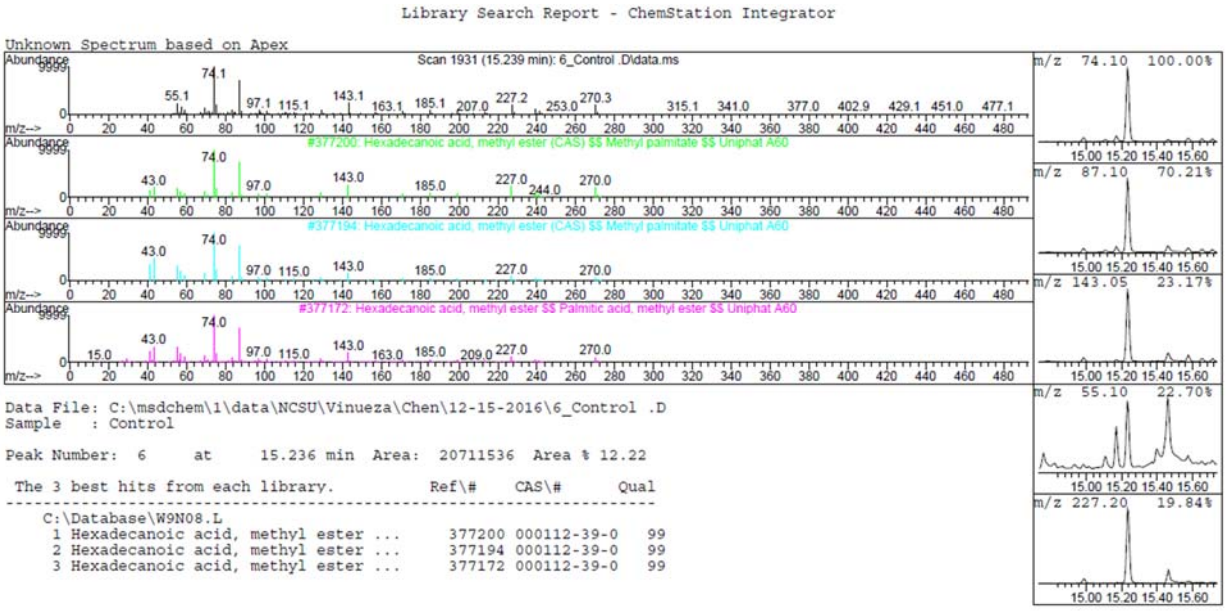

Figure 34 (b) MS spectrum of peak at 15.236 minutes and system match

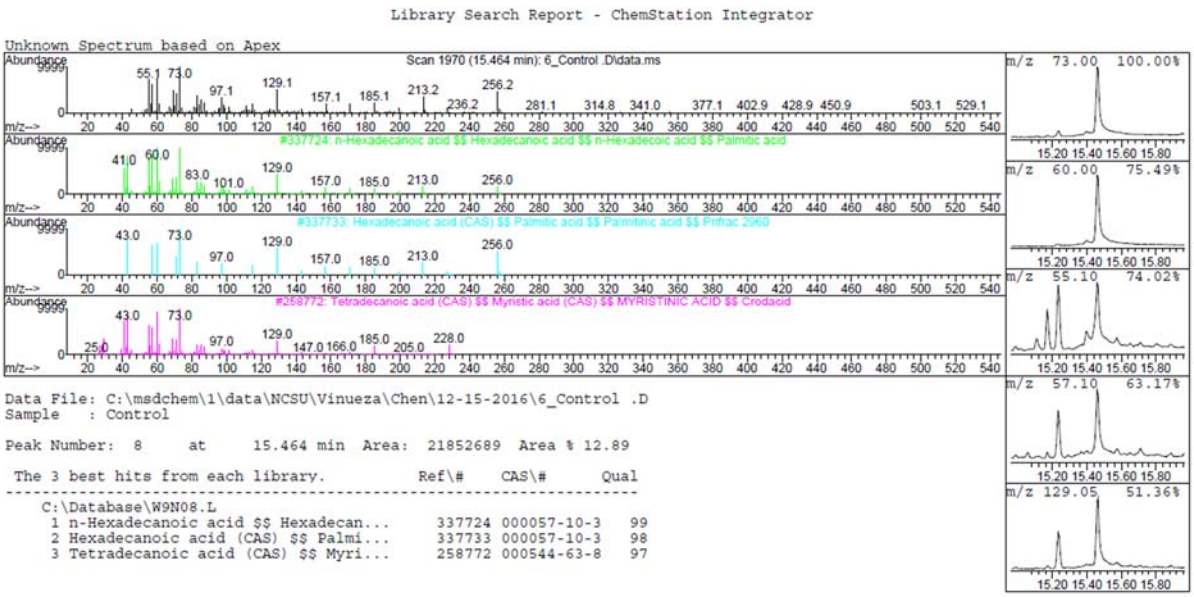

Figure 34 (c) MS spectrum of peak at 15.464 minutes and system match

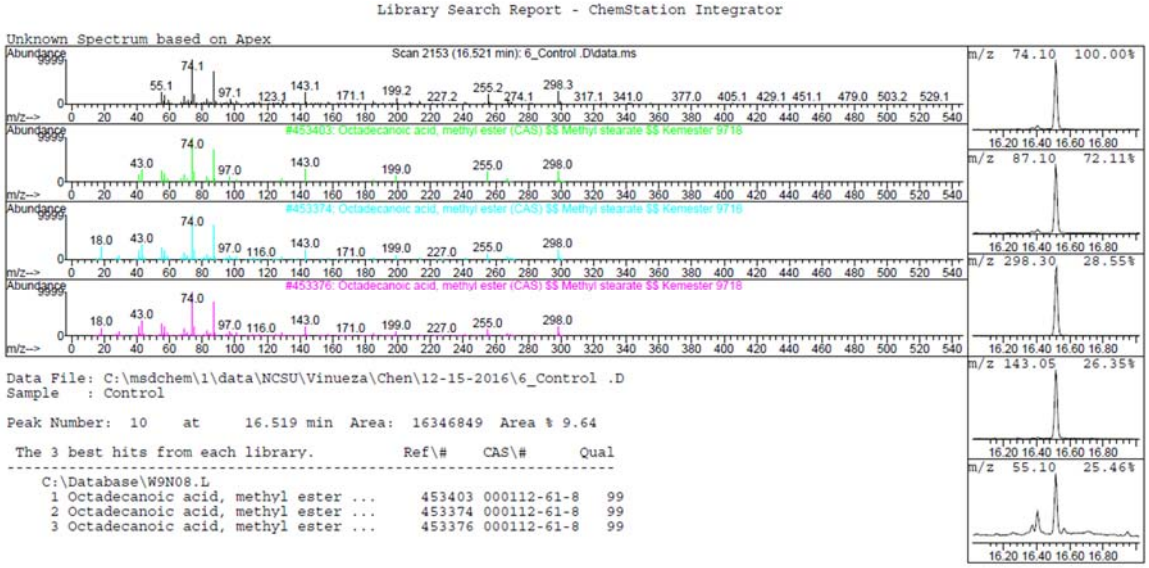

Figure 34 (d) MS spectrum of peak at 16.519 minutes and system match

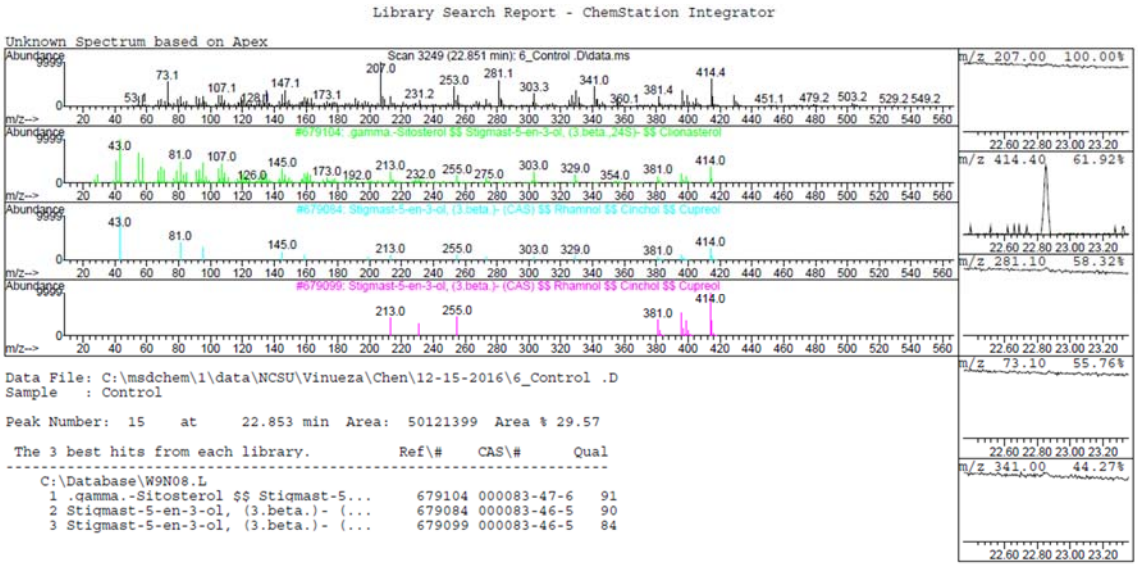

Figure 34 (e) MS spectrum of peak at 22.853 minutes and system match

The GC Chromatogram from the washing liquid of degraded Reactive Yellow 174 fabric is presented in Figure 35 (a). Like the chromatogram from white control, it has a concentration of peaks in retention time ranging from 13 to 17 minutes. It also has a separate peak at 22.842 minutes. Two additional peaks were detected at 10.529 and 12.047 minutes. This suggested that although the white fabrics and the yellow fabrics might have some similarities in their degradation products, the yellow has some unique products.

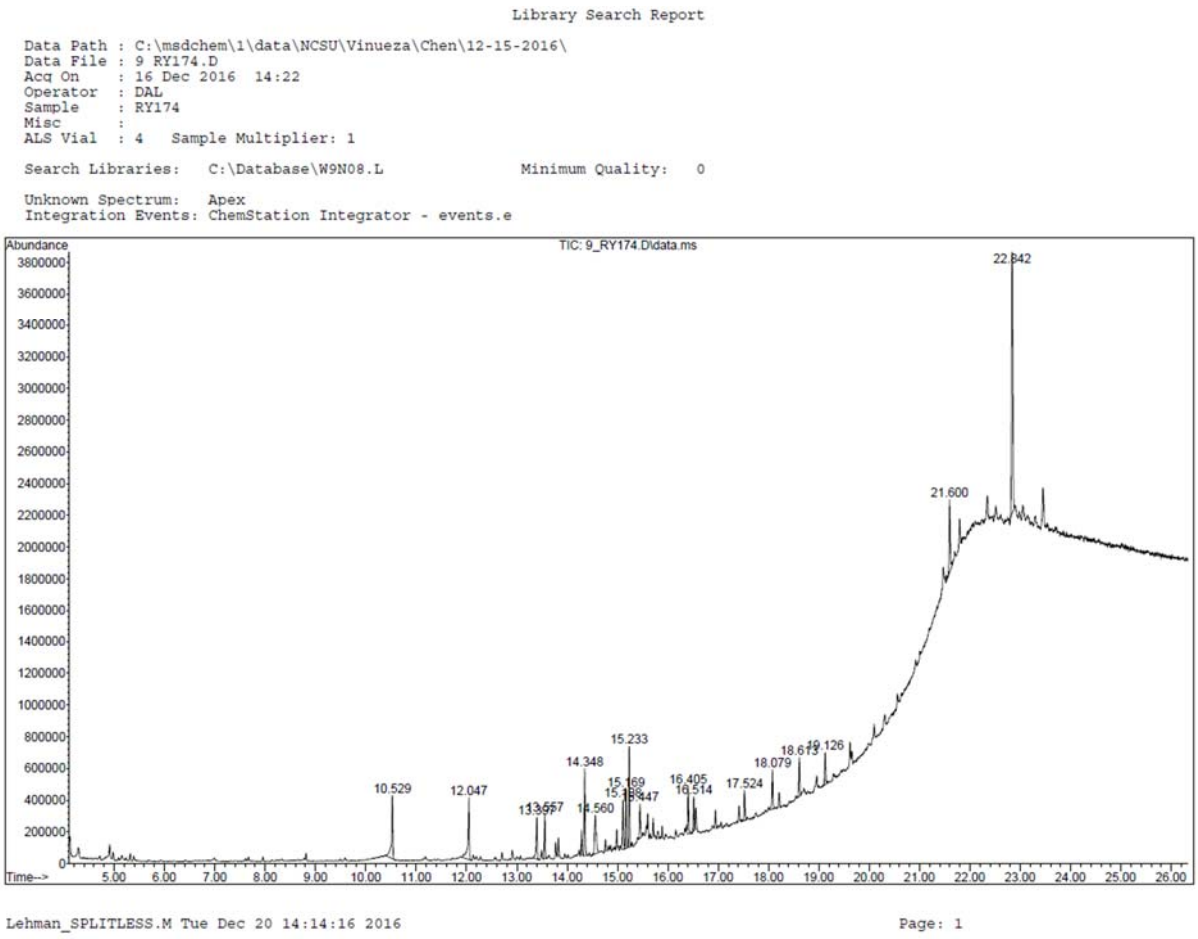

Figure 35 (a) GC Chromatogram of degraded Reactive Yellow 174 fabrics washing liquid

According to the report from GC-MS system, the peak of 14.348 and 15.233 minutes were identified as tetradecanoic acid, 12-methyl-, methyl ester and hexadecanoic acid, methyl ester, respectively. And the peak at 22.842 was identified as beta-sitosterol, which is another kind of planetary steroid like gamma-sitosterol identified in the chromatogram of white fabrics. The additional two peaks at 10.529 and 12.047 minutes were identified on the EI database as dodecamethylcyclohexasiloxane, a kind of silicone compound where silica atoms served as the backbone of its ring structure. Figure 35 (b) to (d) shows the MS of these peaks mentioned

above. It is noticeable that none of these peaks except the peak at 15.233 minutes were identified with a perfect quality, which means that match result from the system may have a certain level of variation from the actual compound.

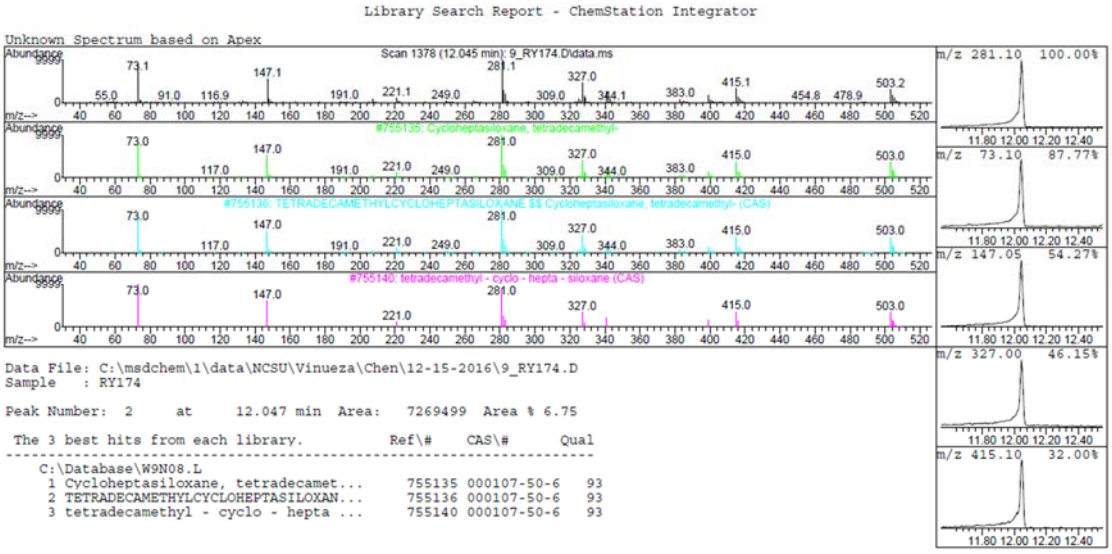

Figure 35 (b) MS spectrum of peak at 12.047 minutes and system match

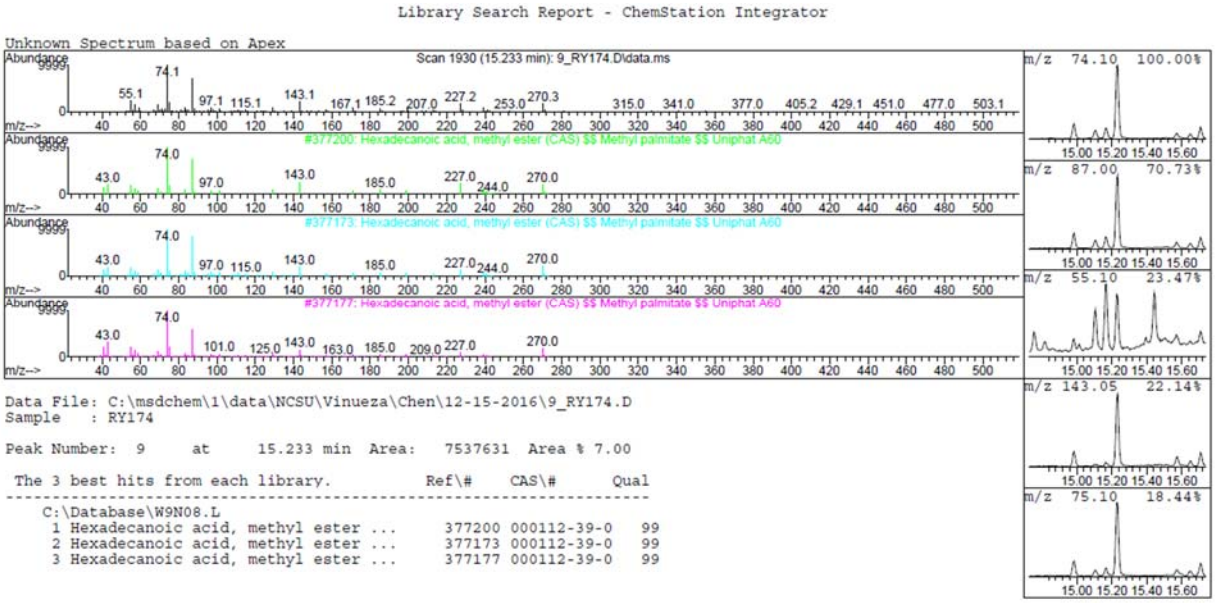

Figure 35 (c) MS spectrum of peak at 15.236 minutes and system match

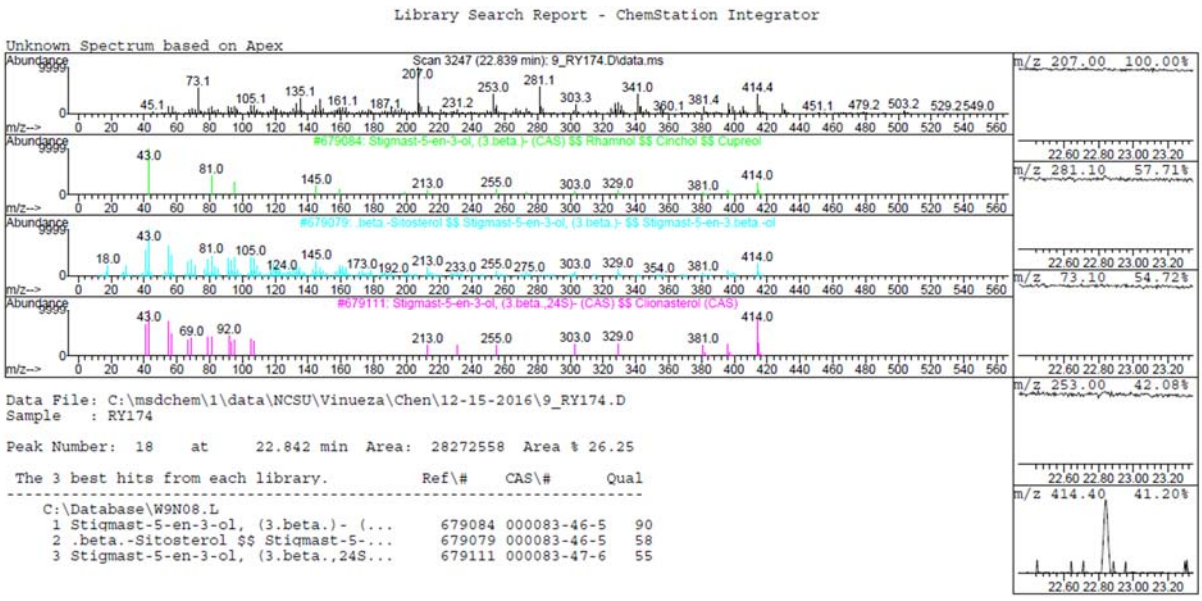

Figure 35 (d) MS spectrum of peak at 22.842 minutes and system match

A table of compounds identified from the chromatogram by the GC-MS system is presented in Table 3. According to this table, there was mainly three type of compounds found in these two washing: fatty acid and its ester, silicone oil derivatives like siloxane, and gamma-Sitosterol. To study the origin of these compounds, the sample history of these fabrics was reviewed. According to the procedure report from Cotton Incorporation, in the bleaching process, both of the white and yellow fabrics were treated with hydrogen peroxide as well as a series of textile auxiliaries such as SULTAFON™ D, Marlube™ CMN, and Marquest™ PB. Among them, nonionic surfactant SULTAFON™ D serves as the wetting agent. Marlube™ CMN served as a polymer lubricant between the machine and fabrics. Marquest™ PB will stabilize the peroxide during the bleaching. Based on these information, it is reasonable to conclude that the fatty acid ester and silicone derivatives components detected by GC-MS in the washing liquids of degraded white and yellow fabrics could be traced back to the wetting

agents and lubricants used during the bleaching. The detection of gamma-Sitosterol in the mixture could be accounted by the fact that the soil used in the degradation experiment is originally designed for planetary uses such as gardening and farming, so, it is expected that a plant material presented on the soil could be transferred to the surface of the fabrics as the degradation process progressed .

Table 3 List of all compounds found in degraded fabrics washing liquids

45 Days Degraded Control White Fabrics		45 Days Degraded Reactive Yellow 174 Fabrics	
Compound Name	Quality	Compound Name	Quality
Methyl 13-methyltetradecanoate	99	Cyclohexasiloxane, dodecamethyl-	90
Tetradecanoic acid, 12-methyl-, methyl ester	98	Cycloheptasiloxane, tetradecamethyl-	93
Methyl 13-methyltetradecanoate	98	Cyclooctasiloxane, hexadecamethyl-	62
Pentadecanoic acid	95	pinane/BICYCLO[3.1.1]HEPTANE, 2,6,6-TRIMETHYL-	56
9-Hexadecenoic acid	99	Pentadecanoic acid, methyl ester	94
Hexadecanoic acid	99	Cyclononasiloxane, octadecamethyl-	94
cis-9-Hexadecenoic acid	97	9-Hexadecenoic acid, methyl ester,	99
n-Hexadecanoic acid	99	9-Hexadecenoic acid, methyl ester,	99
11-Octadecenoic acid	99	Hexadecanoic acid, methyl ester	99
Octadecanoic acid, methyl ester	99	9-Octadecenoic acid (Z)-	91
l-Methionine, N-neopentyloxycarbonyl-, dodecyl ester	64	9-Octadecenoic acid (Z)-, methyl ester	99

Table 3 Continued

Nonadecane	42	Octadecanoic acid, methyl ester	99
SILIKONFETT	64	17-n-Hexadecyltetratriacontane	49
SILICONE GREASE, SILICONFETT	45	Octadecane, 1-iodo-	64
gamma.-Sitosterol	91	Octadecyl iodide	50
		Octadecyl iodide	50
		SILIKONFETT	49
		SILIKONFETT	49
		gamma.-Sitosterol	90

5. Conclusion

The result obtained from this research suggested that the two reactive groups on the structure of Reactive Yellow 174 have different reactivity where the monofluorotriazine group is more reactive than the Vinyl Sulfone group. Thus, the hydrolysis of Reactive Yellow dye molecule could be divided into three stages. The first stage of reaction involved the hydrolysis of the monofluorotriazine group and produced a peak of m/z 407.5207 in the mass spectrum. In the next stage of the reaction, this product of m/z 407.5207 got hydrolyzed further on the vinyl sulfone group which produced a peak of 416.5260 m/z. At the last stage of the reaction, the peak of 416.5260 m/z was reduced to 348.5163 m/z by cleaving the vinyl sulfone group from the dye structure at the ether bond.

Regarding the hydrolysis of Reactive Yellow 174 colored fabrics, hydrolysis under alkaline condition was more advantageous than the acid condition since they were able to cleave glucose units from the fabrics as well as remove the dye from the fabrics.

Results from GC-MS analysis suggested that there was still a certain quantity of auxiliaries left on the fabrics after the degradation since most of the compounds identified by the database could trace back to the wetting agents and detergents that were introduced during the production process.

6. Future works

Based on the result from this study, one part of the future work will be focused on the development of an enzymatic method to cleave the fabrics. Because of the efficiency specificity of enzyme towards the glycosidic bond, it is expected that the product will have a structure where the reactive dye is bonded to one or multiple glucose units. Meanwhile, synthesis reaction will be performed to synthesize this type of dye-sugar compound as standard.

Another future direction of this study is the analysis of soil. There is a chance that some of the degradation product or even the dye has leached to the soil, so an extraction method will be developed to extract dye from the soil.

REFERENCES

1. Tappe, H.; Helmling, W.; Mischke, P.; Rebsamen, K.; Reiher, U.; Russ, W.; Schläfer, L.; Vermehren, P. In *Reactive Dyes;* Ullmann's Encyclopedia of Industrial Chemistry; Wiley-VCH Verlag GmbH & Co. KGaA: 2000; .

2. Zollinger, H., 1919-2005 *Color chemistry : syntheses, properties, and applications of organic dyes and pigments;* Verlag Helvetica Chimica Acta; Wiley-VCH: Zürich; Weinheim, 2003; .

3. Lewin, M. *Handbook of Fiber Chemistry;* CRC Press: Boca Raton, 2007; Vol. 3rd ed.

4. Watson, J. T. *Introduction to mass spectrometry electronic resource] : instrumentation, applications and strategies for data interpretation;* John Wiley & Sons: Chichester, England ; Hoboken, NJ, 2007; .

5. Griffiths, J. A brief history of mass spectrometry. *Anal. Chem.* **2008**, *80*, 5678-5683.

6. Thomson, J. J. (. *Recollections and reflections;* New York, Macmillan, 1937: 1937; .

7. , Proceedings of the American Physical Society. *Phys. Rev.* **1946**, *69*, 674.

8. GUILHAUS, M. PRINCIPLES AND INSTRUMENTATION IN TIME-OF-FLIGHT MASS-SPECTROMETRY - PHYSICAL AND INSTRUMENTAL CONCEPTS. *JOURNAL OF MASS SPECTROMETRY* **1995**, *30*, 1519-1532.

9. Kingdon, K. H. A Method for the Neutralization of Electron Space Charge by Positive Ionization at Very Low Gas Pressures. *Physical Review* **1923**, *21*, 408-418.

10. Makarov, A. Electrostatic axially harmonic orbital trapping: A high-performance technique of mass analysis. *Anal. Chem.* **2000**, *72*, 1156-1162.

11. Shi, S. D. -.; Hendrickson, C. L.; Marshall, A. G. Counting individual sulfur atoms in a protein by ultrahighresolution Fourier transform ion cyclotron resonance mass spectrometry: Experimental resolution of isotopic fine structure in proteins. *Proc. Natl. Acad. Sci. U. S. A.* **1998**, *95*, 11532-11537.

12. Dass, C. *Fundamentals of contemporary mass spectrometry;* Wiley-Interscience: Hoboken, N.J., 2007; .

13. Gross, J. H. *Mass Spectrometry electronic resource] : A Textbook;* Springer Berlin Heidelberg: Berlin, Heidelberg, 2011; .

14. Cameron, A. E.; Eggers, D. F. An Ion ``Velocitron. *Rev. Sci. Instrum.* **1948**, *19*, 605-607.

15. Wiley, W. C.; McLaren, I. H. Time-of-Flight Mass Spectrometer with Improved Resolution. *Rev. Sci. Instrum.* **1955**, *26*, 1150-1157.

16. Mamyrin, B. A.; Shmikk, D. V. Linear mass reflectron. *Zhurnal Ehksperimental'noj i Teoreticheskoj Fiziki* **1979**, *76*, 1500-1505.

17. deHoffmann, E. Tandem mass spectrometry: A primer. *JOURNAL OF MASS SPECTROMETRY* **1996**, *31*, 129-137.

18. Anonymous *Compendium of chemical terminology : IUPAC recommendations;* Blackwell Science: Oxford Oxfordshire] ; Malden, MA, 1997; .

19. Anonymous *High performance liquid chromatography : fundamental principles and practice;* Blackie Academic & Professional: London ; New York, 1996; .

20. Skoog, D. A. *Principles of instrumental analysis;* Thomson Brooks/Cole: Belmont, CA, 2007; .

21. McMaster, M. C. *HPLC, a practical user's guide;* Wiley-Interscience: Hoboken, N.J., 2007; .

22. Pellew, C. E., author. *Dyes and dyeing;* Abhishek Publications: Chandigarh, 2007; .

23. Clark, M. Handbook of Textile and Industrial Dyeing, Volume 1 - Principles, Processes and Types of Dyes.

24. Upadhyay, S. K. *Chemical kinetics and reaction dynamics;* Springer; Anamaya: New York; New Delhi, India, 2006; .

25. Luttringer, J. P. Cibacron C -- a New Generation of Reactive Dyes for Cotton. *Book of Papers, AATCC International Conference & Exhibition* **1992**, 318.

26. Park, S.; Baker, J. O.; Himmel, M. E.; Parilla, P. A.; Johnson, D. K. Cellulose crystallinity index: measurement techniques and their impact on interpreting cellulase performance. *Biotechnology for Biofuels* **2010**, *3*, 10.

27. Olson, E. S. *Textile wet processes;* Noyes Publications: Park Ridge, N.J., U.S.A., 1983; .

28. Anonymous *Cellulose chemistry and its applications;* E. Horwood; Halsted Press: Chichester, West Sussex, England; New York, 1985; .

29. Sugano, Y.; Matsushima, Y.; Tsuchiya, K.; Aoki, H.; Hirai, M.; Shoda, M. Degradation pathway of an anthraquinone dye catalyzed by a unique peroxidase DyP from Thanatephorus cucumeris Dec 1. *Biodegradation* **2009***, 20*, 433-440.

30. Wiggins, K. G.; Holness, J. A.; March, B. M. The importance of thin layer chromatography and UV microspectrophotometry in the analysis of reactive dyes released from wool and cotton fibers. *J. Forensic Sci.* **2005***, 50*, 364-368.

31. Berns, R. S., 1954- *Billmeyer and Saltzman's principles of color technology;* Wiley: New York, 2000; .

APPENDICES

Appendix A

Structure of all hydrolysis product from Reactive Yellow 174

Reactive Yellow 174

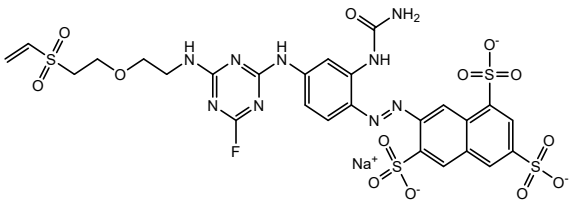

Chemical Formula: $C_{26}H_{23}FN_9NaO_{13}S_4^{2-}$
Exact Mass: 839.0191
m/z: 419.5095

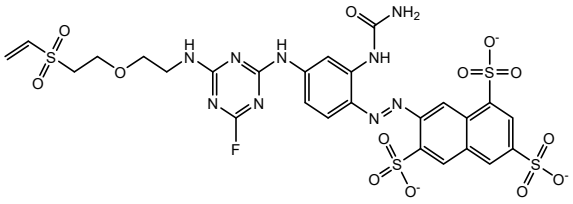

Chemical Formula: $C_{26}H_{23}FN_9O_{13}S_4^{3-}$
Exact Mass: 816.0299
m/z: 272.0100 (100.0%)

Reactive Yellow 174 Hydrolysis at MFT group

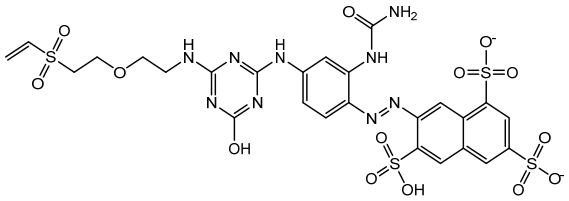

Chemical Formula: $C_{26}H_{25}N_9O_{14}S_4^{2-}$
Exact Mass: 815.0415
m/z: 407.5207

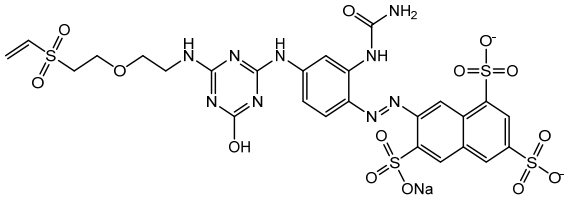

Chemical Formula: $C_{26}H_{24}N_9NaO_{14}S_4^{2-}$
Exact Mass: 837.0234
m/z: 418.5117

Reactive Yellow 174 Hydrolysis at MFT+VS group

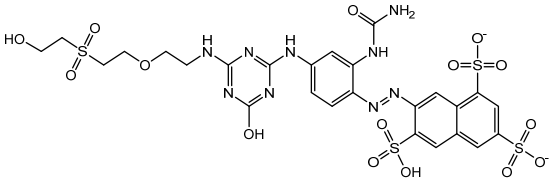

Chemical Formula: $C_{26}H_{27}N_9O_{15}S_4^{2-}$
Exact Mass: 833.0520
m/z: 416.5260

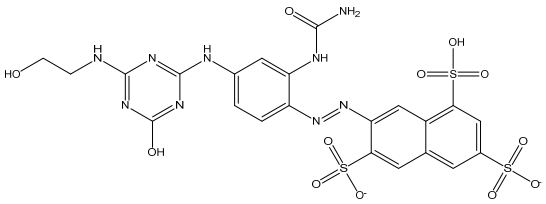

Chemical Formula: $C_{22}H_{19}N_9O_{12}S_3^{2-}$
Exact Mass: 697.0326
m/z: 348.5163

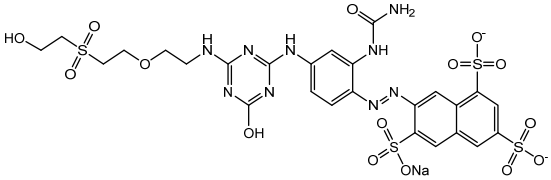

Chemical Formula: $C_{26}H_{26}N_9NaO_{15}S_4^{2-}$
Exact Mass: 855.0340
m/z: 427.5170